論文 / 著書情報
Article / Book Information

題目(和文)	
Title(English)	Analysis of genes responsible for lung metastasis of murine osteosarcoma
著者(和文)	PONGSUCHARTM
Author(English)	Mongkol Pongsuchart
出典(和文)	学位:博士(工学), 学位授与機関:東京工業大学, 報告番号:甲第10975号, 授与年月日:2018年9月20日, 学位の種別:課程博士, 審査員:近藤 科江,丸山 厚,中村 浩之,西山 伸宏,小倉 俊一郎
Citation(English)	Degree:Doctor (Engineering), Conferring organization: Tokyo Institute of Technology, Report number:甲第10975号, Conferred date:2018/9/20, Degree Type:Course doctor, Examiner:,,,,
学位種別(和文)	博士論文
Type(English)	Doctoral Thesis

Tokyo Institute of Technology

Graduate School of Bioscience and Biotechnology

Department of Biomolecular Engineering

Kondoh Laboratory

Analysis of genes responsible for lung metastasis of murine osteosarcoma

Mongkol Pongsuchart

Academic advisor (main): Prof. Shinae Kondoh

Academic advisor (sub): Prof. Atsushi Maruyama

Table of Contents

Chapter 1 General introduction 7

1-1. Osteosarcoma and lung metastasis 8

1-2. Overview of the metastatic process 9

1-2-1. Invasion and Epithelial to mesenchymal transition (EMT) 9

1-2-2. Extravasation step 11

1-2-3. Colonization of the cancer cell at metastatic site 12

1-3. Study of metastatic mechanism by using *in vivo* bioluminescence (BL) imaging. 12

References 14

Chapter 2 Identification of CYGB as a downstream effector of LEF1 16

Abstract 17

2-1. Introduction 18

2-1-1. Establishment of osteosarcoma LM8 sublines with different metastatic ability 18

2-1-2. Identification of gene responsible for lung metastasis in osteosarcoma 21

2-1-3. Genome-wide meta-analysis 25

2-1-4. Lymphoid enhancer factor 1 (LEF1) 27

2-1-5. Cytoglobin 27

2-2. Materials and methods 28

2-2-1. Cell culture 28

2-2-2. Genome-wide meta-analysis 28

2-2-3. qPCR and RT-PCR 28

2-2-4. Western blotting 30

2-2-5. Cell proliferation assay 30

2-3. Results 31

2-3-1. Gene screening by a genome-wide meta-analysis 31

2-3-2. Establishment of CYGB overexpressing and *Cygb* knock out cell line. 36

Discussion 38

References 39

Chapter 3 Analysis of function of CYGB in the extravasation of the LM8 sublines 43

Abstract 44

3-1. Introduction 45

3-1-1. Characterization of metastatic phenotypes in the LM8 sublines 45

3-1-2. Function of LEF1 in lung metastasis in the LM8 sublines 47

3-1-3. Function of CYGB on lipid oxidation 48

3-1-4. Role of NO in cancer progression 48

3-2. Materials and methods....49
3-2-1. Cell culture 49
3-2-2. Establishment of an LM8 cell line with stable CYGB overexpression ...49
3-2-3. Construction of LM8-H/*Cygb*- KO subline by using CRISPR-Cas9 system 50
3-2-4. Vector construction 50
3-2-5. Extravasation assay 50
3-2-6. Cell adhesion assay 52
3-2-7. Transmigration assay 52
3-2-8. Analysis of nitric oxide levels in the LM8 sublines....53
3-2-9. Measurement of arachidonic acid 54

3-3. Results....55
3-3-1. Functions of CYGB in adhesion and transmigration abilities *in vitro* ...55
3-3-2. Effect of NO on CYGB function in extravasation ability of the LM8 sublines 56
3-3-3. Function of CYGB at AA level in the LM8 sublines. 57

Discussion 59

References....63

Chapter 4 Functions of *Cygb* on lung-metastatic ability of the LM8 sublines *in vivo*. 66

Abstract....67

4-1. Introduction 68
4-1-1. Functions of LEF1 on lung metastasis ability of the LM8 sublines *in vivo* 68
4-1-2. Molecular mechanisms of intravasation and extravasation processes ...70

4-2. Materials and methods....72
4-2-1. Mice....72
4-2-2. *In vivo* and *ex vivo* BL imaging....72
4-2-3. Lung metastasis assay 72
4-2-4. Histology analysis 72
4-2-5. Statistical analysis....73

4-3. Results....74
4-3-1. Functions of CYGB on lung metastasis *in vivo* 74

Discussion 78

References....79

Chapter 5 Conclusion remarks and future perspectives 80

Achievements 83

Acknowledgement...84

Abbreviations

AA: Arachidonic acid

BL: Bioluminescence

CDC42: Cell division control protein 42

cDNA: Complementary DNA

CRISPR-Cas9: Clustered regularly interspaced short palindromic repeats associated endonuclease 9

CYGB: Cytoglobin

CYGB-OE: CYGB-overexpressing LM8-L

DDX58: Retinoic acid-inducible gene I protein

DMEM: Dulbecco's Modified Eagle Medium

E-selectin: Endothelial selectin

EMT: Epithelial to mesenchymal transition

FBS: Fetal bovine serum

GSEA: Gene set enrichment analysis

HE: Hematoxylin and eosin

HIF-1α: Hypoxia inducible factor-1α

ID mice: Immune-deficient mice

KO: Knockout

LEF1: Lymphoid enhancer factor 1

MCS: Multi-cloning sites

NF-κB: Nuclear factor kappa-light chain enhancer of activated B cells

NO: Nitric oxide

OE: Overexpression

OS: Osteosarcoma

qPCR: quantitative polymerase chain reaction

RAC1: Ras-related C3 botulinum toxin substrate 1

RhoA: Ras homolog gene family, member A

RT-PCR: Reverse transcription polymerase chain reaction

sLe^a: Sialyl Lewis a

sLe^x: Tetra-saccharide sialyl Lewis x

TCF: T-Cell-Specific Transcription Factor

TGF-β: Transforming growth factor‑β

WST-1: Water-soluble tetrazolium salt 1

Chapter 1
General introduction

1-1. Osteosarcoma and lung metastasis

Osteosarcoma is the most common malignant bone tumor found in both children and adult. Osteosarcoma mostly found in the bones round the knee. In some cases, osteosarcoma also arises in other regions such as radial bone, humerus and pelvis. Overall incidence of osteosarcoma is 3.1 per million per year. The incidence of osteosarcoma is 4.4 per million population per year in patients with the age of 0–24 years (Figure 1-1)[1–3]. Surgical and chemotherapeutic strategies have significantly improved survival rate in osteosarcoma patient in last decade. Five-year survival rate for patients with localized disease is approximately 70%[4, 5]. However, metastatic disease can prevent long-term cure and decrease 5-year survival rate to less than 40%[5]. The lung is the most common site for metastasis in osteosarcoma[6].

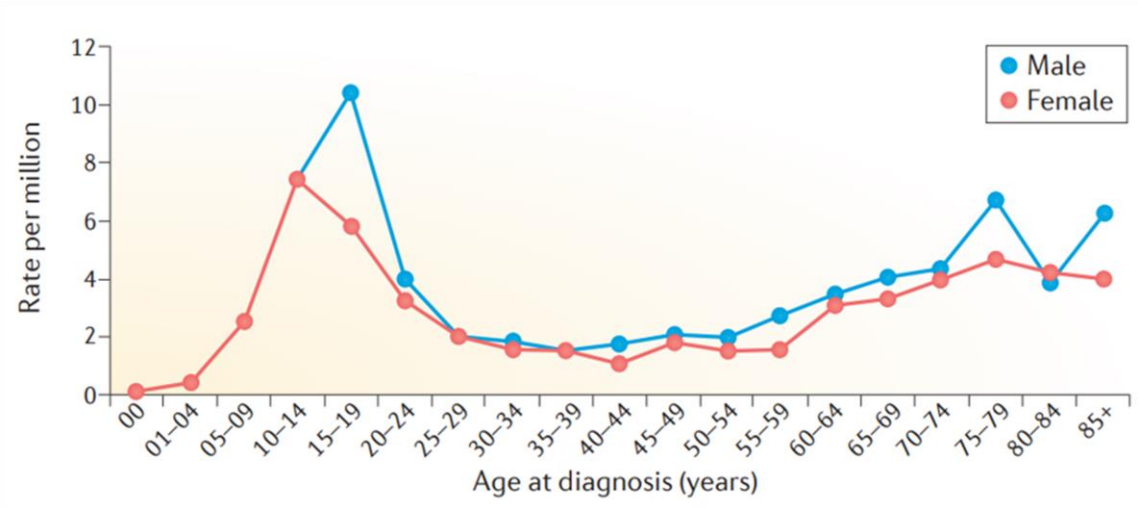

Figure 1-1. Incidence of osteosarcoma per million population. The figure was cited from reference 3.

Although lung metastasis is a major cause of poor prognosis in osteosarcoma patients, effective therapeutic strategies have not been developed. Therefore, there is high demand for developing new therapeutic strategies based on molecular mechanisms of osteosarcoma lung metastasis. Increasing knowledge about the mechanisms of lung metastasis will provide new approaches to achieve long-term cure of patients.

1-2. Overview of the metastatic process

Metastasis is a complicated multi-step process including local tumor cell invasion in the primary tumors, intravasation, survival in blood circulation, extravasation into the secondary organs, formation of metastatic lesion[7, 8] During metastasis process, cancer cell rapidly proliferate and invade nearby tissue[7]. Cancer cell invasion related to enhancement of cell motility including activation of ras-related C3 botulinum toxin substrate 1 (RAC1), a member of small GTP binding protein Rho family, and ras homolog gene family, member A (RhoA)[8]. After that, some of the cancer cell invade through blood vasculature and travel to distance organs. During this process, most of cancer cell die from shear stress inside blood vessel and immune response[8]. Survive cancer cell will interact with vascular endothelial cell to extravasate to the secondary organ. This step required adhesion between cancer-endothelial cell and transmigration through blood vessel that cell-cell interaction is critical[7, 8]. After cancer transmigrate through the endothelial barrier, colonization will be occur to form metastatic nodule (Figure 1-2).

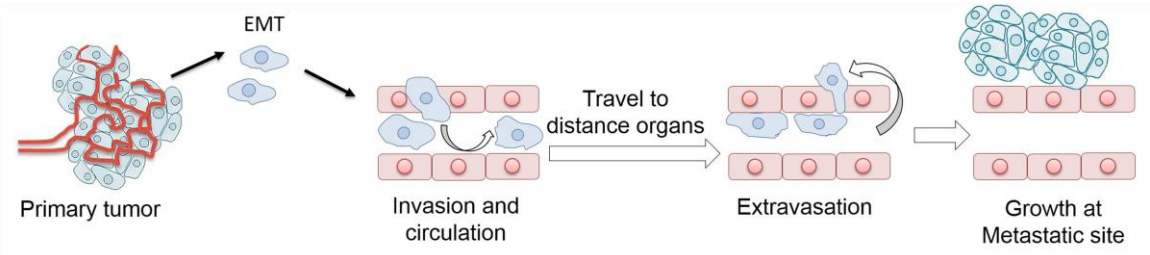

Figure 1-2. Diagram of metastatic process.

1-2-1. Invasion and Epithelial to mesenchymal transition (EMT)

Invasion is a process of direct extension and penetration by cancer cells into neighboring tissues. The proliferation of the cancer cell and the progressive increase in tumor size that leads to a break in the barriers between tissues, leading to tumor extension into adjacent tissue. Local invasion is also the first stage in the process that leads to the development

of secondary tumors or metastases[9]. Two different patterns of invasive growth are; collective cell migration and single cell migration[9]. The migration type is largely determined by tissue microenvironment features and depends on molecular changes in tumor cells[10].

The most common molecular mechanisms that regulated invasion phenotype in collective migration cell are overexpression of E-cadherin and Integrin. For single cell invasion, different sets of gene expression are observed. Down regulation of RAC1 and Integrin, and up-regulation of RhoA were reported[9] (Figure 1-3).

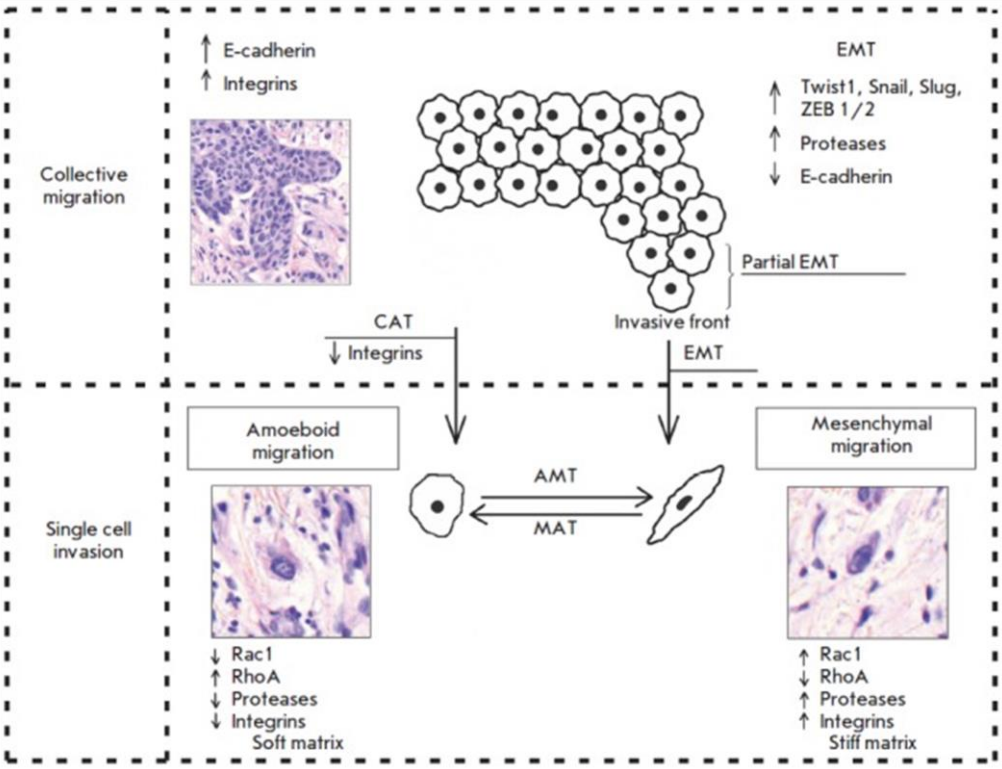

Figure 1-3. Summary diagram of molecular mechanisms that related to invasion step. The figure cited from reference 9.

EMT is an important process that induced epithelial cell to undergo multiple biochemical changes that enable it to mesenchymal cell phenotype. Mesenchymal phenotype enhances migratory capacity, invasiveness, elevated resistance to apoptosis, and greatly increased production of ECM components[11]. EMT is associated with many biological processes such as developmental process, inflammation, and metastasis[12, 13]. During EMT process,

several signaling pathways involving transforming growth factor‑β (TGF-β) AKT and WNT[13, 14] activate genes regulation EMT such as *Slug, Snail, Zeb1, Zeb2,* and *Twist*[14] (Figure 1-4). During this process, loss of epithelial markers can be observed while mesenchymal markers such as Vimentin, Fibronectin, Type I collagen are increased.

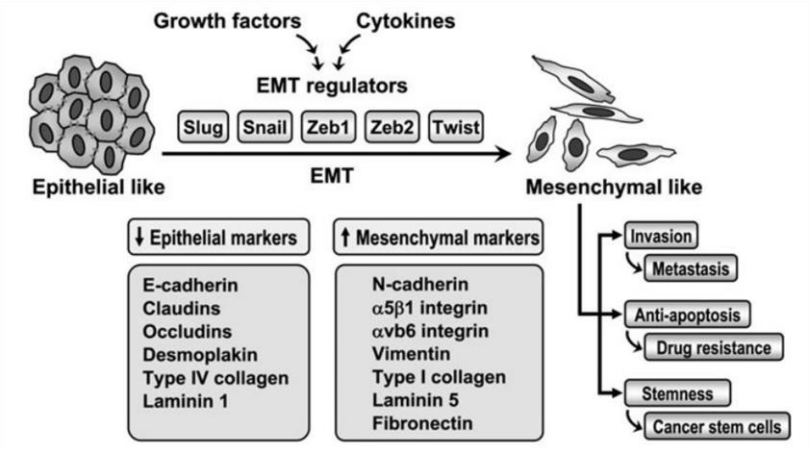

Figure 1-4. Summary diagram of EMT process. The figure was cited from reference 14.

1-2-2. Extravasation step

Extravasation from blood vessels is one of the important steps in the metastatic process. In extravasation, cells have to attach vascular endothelial cells and penetrate the vascular wall to invade secondary organs. In this step, multiple molecules might be involved in interactions between cancer cells and vascular endothelial cells[8, 15]. Previous studies have described that activation of RAC1 in cancer cells promoted cell adhesion ability to endothelial cells[16, 17]. In addition, cell division control protein 42 (CDC42) loose cell-cell junction of vascular endothelial cells though activation of several signaling pathways, enabling cancer cells to penetrate through an endothelial barrier[8, 18]. Extensive studies have identified many cell-surface molecules which play important roles in extravasation of cancer cells[15, 19, 20] (Table 1-1). However, critical regulators are still unknown in osteosarcoma extravasation to the lung[21].

Table 1-1. Endothelial cell adhesion molecules and counter-receptors in cancer cell.

Endothelial cell surface molecules	Cancer cell counter-receptor
Selectins/Lectins	
E-selectin	SLe^A-, SLe^X-glycoproteins
P-selectin	SLe^A-, SLe^X-glycoproteins
Galectin 3	TF-antigen glycoproteins; Mucin 1(MUC1)
Immunoglobulins	
ICAM1	α4β1 (VLA4); MUC1
VCAM1	CD44
L1	αvβ3
Integrins	
α4β1	VCAM1; CD44
α6β1	α6β1; α6β4
Others	
Chloride Channel Accessory (CLCA)	α6β4

The table has been modified from reference 8.

1-2-3. Colonization of the cancer cell at metastatic site

After the cancer cells successfully extravasate through vascular endothelial cell, they can proliferate and form new colonies at the metastatic site and secrete many molecules such as matrix metalloproteinases (MMPs) and cathepsins to support colonization[21, 22]. Moreover, cytokines such as C-X-C Motif Chemokine Ligand 12 (CXCL12)[23] are secreted to support metastatic niche formation.

1-3. Study of metastatic mechanism by using *in vivo* bioluminescence (BL) imaging.

To study molecular mechanisms governing metastasis of cancer cells, *in vivo* BL imaging technique has been used to isolate and characterize metastatic subpopulation derived from parental cell lines[24, 25]. Briefly, luciferase expressing cancer cells were injected into the blood stream of mice. Bioluminescence imaging allowed us to noninvasively monitor

metastatic growth of cancer cells and precisely collect cancer cells from metastatic sites for culturing *in vitro*. Expanded cancer cells were then injected again into mice. After repeating these processes several times, highly metastatic cell lines were established. Striking example of the study using such high metastatic cell lines is that comparative genetic analysis between of human breast cancer cell lines with high metastatic ability and their parental cell lines successfully identified a small gene subset (*Id1*, *Cxcl1*, *Ptgs2*, *Mmp1*, *Sparc* and *Mmp2*) highly responsible for metastasis to the lung[26].

References

1. Savage S, Mirabello L. Using epidemiology and genomics to understand osteosarcoma etiology. *Sarcoma* 2011; 2011: 1–13.
2. Yang G, Yuan J, Li K. EMT transcription factors: implication in osteosarcoma. *Med Oncol* 2013; 30: 1–5.
3. Gianferante DM, Mirabello L, Savage SA. Germline and somatic genetics of osteosarcoma - connecting aetiology, biology and therapy. *Nat Rev Endocrinol* 2017; 13: 480–491.
4. Aljubran AH, Griffin A, Pintilie M, et al. Osteosarcoma in adolescents and adults: survival analysis with and without lung metastases. *Ann Oncol* 2009; 20: 1136–1141.
5. Isakoff MS, Bielack SS, Meltzer P, et al. Osteosarcoma: Current Treatment and a Collaborative Pathway to Success. *J Clin Oncol* 2015; 33: 3029–3035.
6. Saha D, Saha K, Banerjee A, et al. Osteosarcoma relapse as pleural metastasis. *South Asian J Cancer* 2013; 2: 56–59.
7. Hunter KW, Crawford NPS, Alsarraj J. Mechanisms of metastasis. *Breast Cancer Res* 2008; 10 Suppl 1: S2.
8. Reymond N, d'Agua BB, Ridley AJ. Crossing the endothelial barrier during metastasis. *Nat Rev Cancer* 2013; 13: 858–870.
9. Katja B, Claudia M, Jürgen B. Expression profiling reveals genes associated with transendothelial migration of tumor cells: A functional role for αvβ3 integrin. *Int J Cancer* 2007; 121: 1910–1918.
10. Scott RW, Crighton D, Olson MF. Modeling and Imaging 3-Dimensional Collective Cell Invasion. *J Vis Exp* 2011; 3525:1-5.
11. Nakaya Y, Sheng G. EMT in developmental morphogenesis. *Cancer Lett* 2013; 341: 9–15.
12. López‐Novoa JM, Nieto MA. Inflammation and EMT: an alliance towards organ fibrosis and cancer progression. *EMBO Mol Med* 2009; 1: 303–314.
13. Huber MA, Azoitei N, Baumann B, et al. NF-κB is essential for epithelial-mesenchymal transition and metastasis in a model of breast cancer progression. *J Clin Invest* 2004; 114: 569–581.

14. Shih J-Y, Yang P-C. The EMT regulator slug and lung carcinogenesis. *Carcinogenesis* 2011; 32: 1299–1304.
15. Miles FL, Pruitt FL, Van Golen KL, et al. Stepping out of the flow: Capillary extravasation in cancer metastasis. *Clin Exp Metastasis* 2008; 25: 305–324.
16. Naikawadi RP, Cheng N, Vogel SM, et al. A Critical Role for Phosphatidylinositol (3,4,5)-Trisphosphate–Dependent Rac Exchanger 1 in Endothelial Junction Disruption and Vascular Hyperpermeability. *Circ Res* 2012; 111: 1517–1527.
17. Tan W, Palmby TR, Gavard J, et al. An essential role for Rac1 in endothelial cell function and vascular development. *FASEB J* 2008; 22: 1829–1838.
18. Reymond N, Im JH, Garg R, et al. Cdc42 promotes transendothelial migration of cancer cells through β1 integrin. *J Cell Biol* 2012; 199: 653–668.
19. Tantivejkul K, Kalikin LM, Pienta KJ. Dynamic process of prostate cancer metastasis to bone. *J Cell Biochem* 2004; 91: 706–717.
20. Mendonsa AM, VanSaun MN, Ustione A, et al. Host and tumor derived MMP13 regulate extravasation and establishment of colorectal metastases in the liver. *Mol Cancer* 2015; 14: 1–12.
21. Kessenbrock K, Plaks V, Werb Z. Matrix Metalloproteinases: Regulators of the Tumor Microenvironment. *Cell* 2010; 141: 52–67.
22. Quail DF, Joyce JA. Microenvironmental regulation of tumor progression and metastasis. *Nat Med* 2013; 19: 1423-37.
23. Müller A, Homey B, Soto H, et al. Involvement of chemokine receptors in breast cancer metastasis. *Nature* 2001; 410: 50-56.
24. Asai T, Ueda T, Itoh K, et al. Establishment and characterization of a murine osteosarcoma cell line (LM8) with high metastatic potential to the lung. *Int J Cancer* 1998; 76: 418–422.
25. Kha NT. Identification of genes responsible for lung metastasis of osteosarcoma by using in vivo image-guided screening system. Master thesis. Graduate School of Bioscience and Biotechnology, Tokyo Institute of Technology, 2014.
26. Minn AJ, Gupta GP, Siegel PM, et al. Genes that mediate breast cancer metastasis to lung. *Nature* 2005; 436: 518–524.

Chapter 2
Identification of CYGB as a downstream effector of LEF1

Abstract

Previous study revealed that transcription factor LEF1 plays an important role in lung metastasis in the LM8 sublines by promoting extravasation ability of LM8-H cell. To identify downstream effectors of LEF1 that are involved in OS lung metastasis, 13 genes were selected based on the LM8 microarray data and genome-wide meta-analysis of a public database for OS patients. Among of them, expression level of Cytoglobin (*Cygb*) is well-correlated with expression of LEF1. Transcription factor binding site prediction suggested that LEF1 can directly bind to the promoter region of *Cygb*. In addition, knockout of *Cygb* in LM8-H significantly increased proliferation rate compared to LM8-H whereas overexpressing of CYGB showed the opposite effect. These results are similar to those obtained when the expression level of LEF1 is reduced and overexpressed, respectively. Taken together, these results suggested that CYGB is a downstream effector of LEF1.

2-1. Introduction

2-1-1. Establishment of osteosarcoma LM8 sublines with different metastatic ability

LM8 is a highly lung-metastatic murine osteosarcoma cell line[1]. In the previous study, LM8 cells with high metastatic ability to the bone and low metastatic ability to the lung has been established by an image-guided *in vivo* BL screening system[2]. Briefly, LM8 stably expressing firefly luciferase (LM8/luc) were intracardially injected into immune-deficient (ID) mice. Metastasis formation was monitored weekly by whole body imaging using IVIS. At day 14, LM8 cells metastasized to the hind limbs were collected from the bone and cultured. The LM8 cells expanded were transplanted into ID mice and collected cancer cells from bone metastasis tissue again. This procedure was repeated 3 more times and an LM8 subline, named LM8-L, that almost completely lost pulmonary metastatic ability was established. Then, LM8-L was then orthotopically injected into the tibia of ID mice. Bioluminescent signal from lung metastasis were detected at 2 weeks after injection. The metastasized lung tissue was collected and minced tissues were cultured with a G418-conaining selection medium to isolate LM8 cells. A high metastatic LM8 subline was successfully isolated from the lung and was named LM8-H (Figure 2-1).

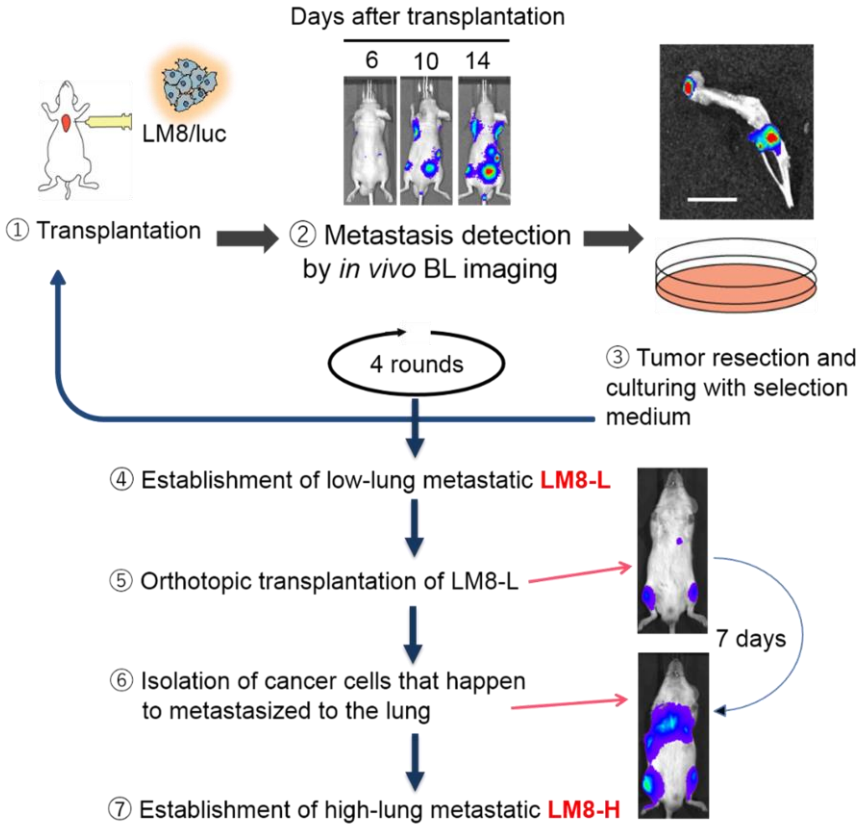

Figure 2-1. Diagram of establishment of non-lung metastatic and lung metastatic LM8 sublines. The figure was cited from reference 2 with slight modification.

BL signal in the lung was significantly higher in the mice injected with LM8-H compared to those injected with LM8-L (Figure 2-2). Histological analysis of the lung was confirmed that LM-H developed significantly more metastatic foci than LM8-L (Figure 2-3). When the LM8 sublines were subcutaneously injected to mice, the growth of LM8-L tumors was faster than that of LM8-H tumors (Figure 2-4), suggesting that the results of Figure 2-3 are not due to the difference in proliferation between the LM8 sublines. In my study, LM8 sublines with high (LM8-H) and low (LM8-L) metastatic ability to the lung were used to identify crucial factors to develop lung metastasis of osteosarcoma.

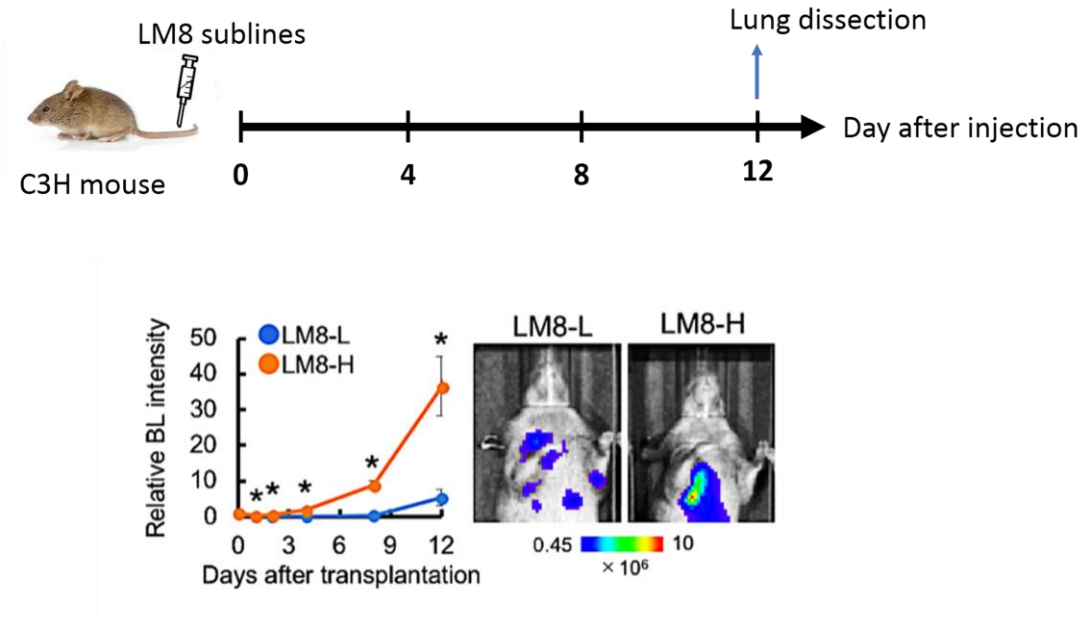

Figure 2-2. Lung metastatic abilities of LM8-L and LM8-H cells. Representative *in vivo* bioluminescence (BL) images on day 12 (right) and quantitative analysis (left) are shown. BL signals from the lungs were normalized to the BL signals on day 0. n = 5, *P < 0.05.

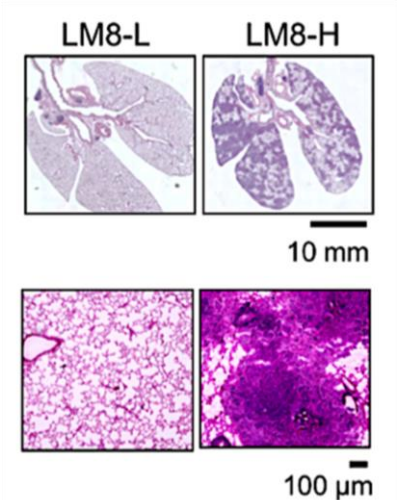

Figure 2-3. Representative HE-stained images of lung tissues at 14 days after injection of LM8 sublines.

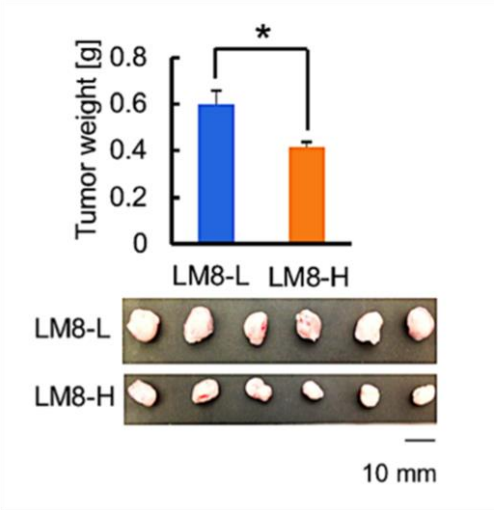

Figure 2-4. Subcutaneous tumor formation. LM8 sublines were injected subcutaneously into C3H mice. The tumors were excised on day 30 (bottom photos). Tumor weights were measured and average values are shown. n = 6. *P < 0.05.

2-1-2. Identification of gene responsible for lung metastasis in osteosarcoma

To identify gene responsible for lung metastasis in the LM8 sublines, gene expression profile (Figure 2-5) and gene set enrichment analysis (GSEA) was performed. GSEA results suggested that LEF1-related genes and several pathways such as AKT and MAPK were enriched in LM8-H cells (Figure 2-6 and Table 2-1). Among the candidate genes, LEF1 was prominent and highly expressed in LM8-H. Differential expression level of LEF1 in the LM8 sublines was confirmed by Western blotting (Figure 2-7).

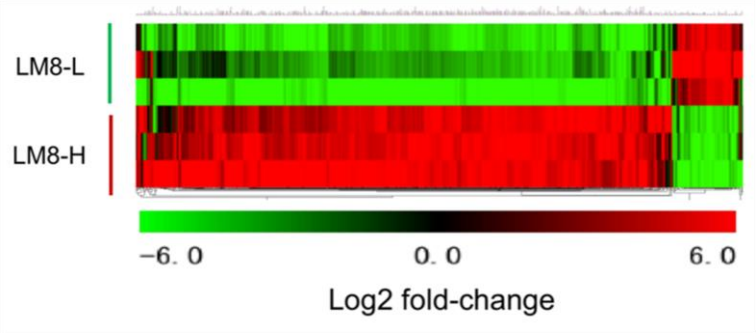

Figure 2-5. A heat map of the DNA microarray analysis data of the LM8 sublines indicated. The heat map shows 500 genes with the greatest differential expression (fold-change > 2) between the LM8-H and LM8-L cells.

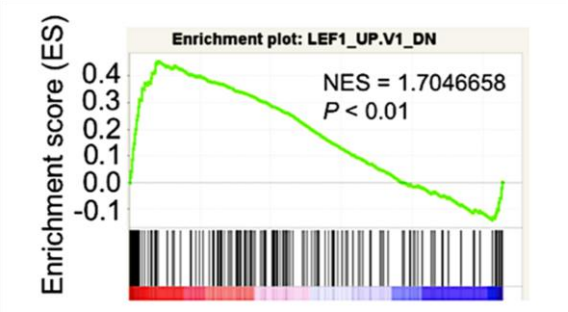

Figure 2-6. Gene set-enrichment analysis of *Lef1* in the LM8 sublines.

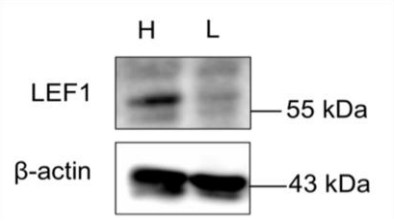

Figure 2-7. LEF1 protein-expression levels in LM8-H (H) and LM8-L (L) cells.

To assess function of LEF1 in lung-metastatic ability of LM8-H cells, *Lef1* knockout (KO) cell lines were established using the clustered regularly interspaced short palindromic repeats (CRISPR)-associated endonuclease 9 (Cas9) system, two independent *Lef1* KO clones (LM8-H/*Lef1*-KO1 and LM8-H/*Lef1*-KO2) were

established using different gRNA (Figure 2-8). When *Lef1* KO clones were intravenously injected into C3H mice, lung metastasis was significantly reduced: KO of *Lef1* significantly suppressed the lung metastasis of LM8-H cells (Figure 2-9).

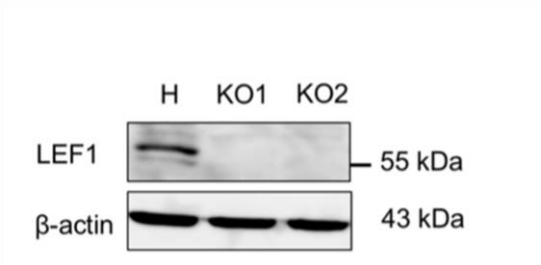

Figure 2-8. Establishment of *Lef1*-KO sublines from LM8-H (H) cells. LEF1 expression in LM8-H/*Lef1*-KO1 (KO1) and LM8-H/*Lef1*-KO2 (KO2) cells was examined by western blotting.

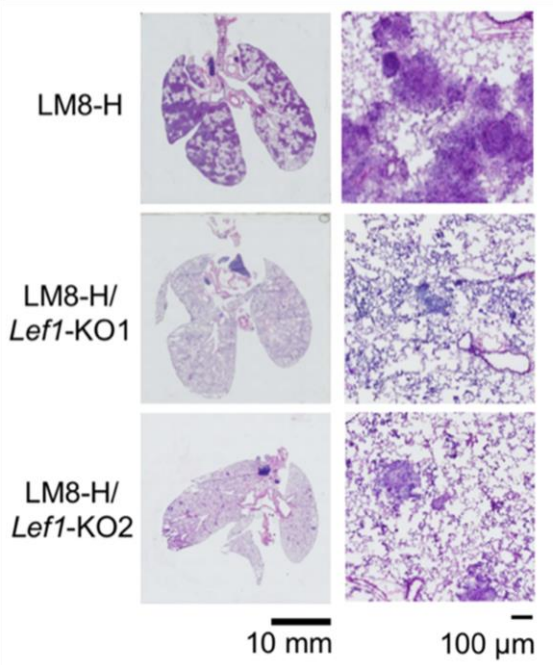

Figure 2-9. Representative HE staining of the lungs at 15 days after intravenous injection of the LM8 sublines.

Table 2-1. List of candidate pathways that enriched in LM8-H from GSEA analysis.

NAME	Geneset description	NES	NOM p-val
LTE2_UP.V1_UP	Genes up-regulated in MCF-7 cells positive for ESR1 and long-term adapted for estrogen-independent growth	1.950429	<0.01
EIF4E_DN	Genes down-regulated in EIF4E overexpressing cells	1.92469	<0.01
AKT_UP_MTOR_DN.V1_UP	Genes up-regulated while AKT1 overexpresssing and mTOR blocking	1.822171	<0.01
RB_P130_DN.V1_DN	Genes down-regulated in RB1 and RBL2 knock out cells	1.790583	<0.01
RAPA_EARLY_UP.V1_DN	Genes up-regulated in lymphoma cells by rapamycin	1.786634	<0.01
ERB2_UP.V1_UP	Genes up-regulated in ESR1 positive and ERBB2 overexpressing cells	1.776906	<0.01
CYCLIN_D1_KE_.V1_UP	Genes up-regulated CCND1 overexpressing cell	1.727938	<0.01
RAF_UP.V1_UP	Genes up-regulated in stably overexpressing RAF1 cells	1.727196	<0.01
MEK_UP.V1_UP	Genes up-regulated in stably overexpressing MAP2K1 cells	1.721152	<0.01
ATF2_S_UP.V1_DN	Genes down-regulated in myometrial cells over-expressing a shortened splice form of ATF2	1.691881	<0.01
MYC_UP.V1_DN	Genes down-regulated in primary epithelial breast cancer cell culture over-expressing MYC	1.684781	<0.01
BMI1_DN_MEL18_DN.V1_UP	Genes up-regulated in DAOY cells (medulloblastoma) upon knockdown of BMI1 and PCGF2	1.682689	<0.01
AKT_UP.V1_UP	Genes up-regulated in mouse prostate by transgenic expression of human AKT1 gene	1.674986	<0.01
TBK1.DF_UP	Genes up-regulated in epithelial lung cancer cell upon over-expression of oncogenic KRAS and knockdown of TBK1	1.673101	<0.01
KRAS.300_UP.V1_DN	Genes down-regulated in four lineages of epithelial cell lines over-expressing an oncogenic form of KRAS	1.636606	<0.01
IL2_UP.V1_UP	Genes up-regulated in Sez-4 cells (T lymphocyte) stimulated with IL2	1.634646	<0.01
P53_DN.V1_UP	Genes up-regulated in NCI-60 panel of cell lines with mutated TP53	1.622398	<0.01
ATM_DN.V1_UP	Genes up-regulated in HEK293 cells (kidney fibroblasts) upon knockdown of ATM	1.614227	<0.01
MTOR_UP.V1_DN	Genes down-regulated by mTOR inhibitor in prostate tissue	1.595322	<0.01

2-1-3. Genome-wide meta-analysis

Meta-analysis is a statistical method for comparing and pooling results from a large date set to find data that commonly shared between data set. In this study, a genome-wide association study meta-analysis was performed using pooled public genome datasets of human osteosarcoma to find common genes that responsible for lung metastasis in murine and human OS[3, 4]. Pool of data set could increase sample size that improves possibility to detect specific associations among genes compared to a single study approach[5]. Indeed, genome-wide meta-analysis successfully identified candidate genes or genetic variation that associated with diseases[6-8]. In addition, this method has been widely used in cancer research field to extract factors related to tumor malignancy and prognosis[9, 10]. For example, analysis of gene expression profiles among various cancer cells and tumor biopsy samples has become a standard approach to survey correlation between expression levels of specific genes and patient prognosis. In this study, the gene expression profiles of the LM8 sublines were combined with the clinical datasets of osteosarcoma patients using a general statistical analysis, p value meta-analysis, used in meta-analysis and other methods (Figure 2-10 and Table 2-2). p value meta-analysis is an easy way to use p value to determine statistical difference among datasets regardless of population size.

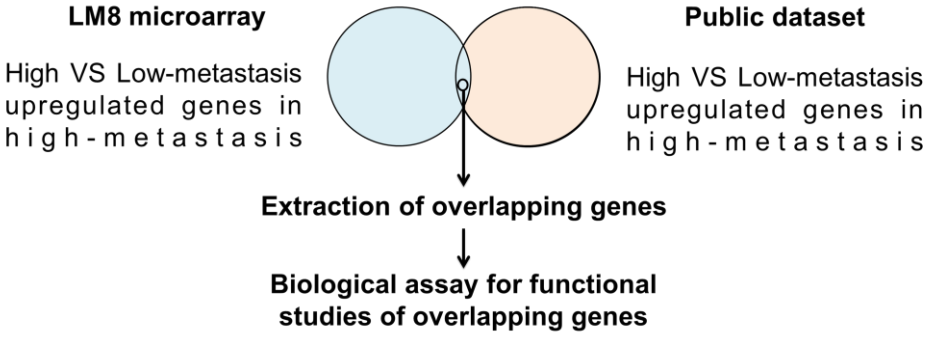

Figure 2-10. Diagram of identification of candidate genes using meta-analysis.

Table 2-2. Summary of methods for meta-analysis of genome-wide data.

Method	Description	Advantages	Disadvantages	Main software used
P value meta-analysis	Simplest meta-analysis approach	Allow meta-analysis when effects are not available	Direction of effect is always available; inability to provide effect sizes; difficulties in interpretation	METAL, GWAMA, R packages
Fixed effects	Synthesis of effect sizes. Between-study variance assume to be zero	Effects readily available through specialized software	Results may be biased if a large amount of heterogeneity existed	METAL, GWAMA, R packages
Random effects	Synthesis of effect sizes. Assume that the individual studies estimate different effects	Generalizability of the results	Power deserts in discovery efforts; may yield spuriously large summary effect estimates when there are selection biases	GWAMA, R packages
Bayesian approach	Incorporate prior assessment of the genetic effects	Most direct method for interpretation of results as posterior probabilities given the observed data	Methodologically challenging; GWAS-tailored routine software not available; subjective prior information used	R packages
Multivariate approach	Incorporate the possible correlation between outcomes or genetic variants	Increased power can identify variants that conventional meta-analysis do not reveals using the same data sets	Computationally intensive; software not available for all analyses; some may require individual-level data	GCTA for multi-locus approaches
Other extensions	A set of different approaches that allow for the identification of multiple variants across different diseases	Summary results of previous meta-analysis can be used	May need additional exploratory analyses for the identification of variants; prone to systematic biases	Software developed by the authors of the proposed methodologies

GCTA, genome-wide complex trait analysis; GWAS, genome –wide association study.

This table was cited from reference 4.

2-1-4. Lymphoid enhancer factor 1 (LEF1)

Lef1 gene encodes LEF1 that has homology with high-mobility group protein (HMG) 1 and contains a HMG-box domain involved in DNA binding[9]. LEF1 is a transcription factor but lacks the ability to initiate transcription by itself; other co-activators or multi-proteins enhancer complexes are necessary to stimulate expression of target genes. LEF1 can also combine with Ally of AML1 and LEF1 and other enhancer binding proteins to regulate expression of the T cell receptor alpha enhancer[12]. Moreover, T-Cell-Specific Transcription Factor /LEF1 is an important complex in Wnt signaling pathway. This complex interacts with β-catenin to regulate target genes of Wnt signaling pathway[13]. A study showed that LEF1 helps metastatic process to the bone of lung adenocarcinoma cells[14]. Recent results suggested that decreased expression of LEF1 suppresses invasion of LM8 cells and human osteosarcoma cell lines[15]. Moreover, knock down *Lef1* and *Notch1* in human osteosarcoma significantly decreased metastasis in mice model[15]. These results support the hypothesis that LEF1 is an important player in lung metastasis of LM8. However, downstream targets of LEF1 that promote lung metastasis have not been identified as well as the upstream mechanism of LEF1 regulation in osteosarcoma.

2-1-5. Cytoglobin

Cytoglobin (CYGB) is a member of the globin family of proteins, which include hemoglobin and myoglobin[16, 17]. *Cygb* was first identified as an inflammatory- and fibrosis-related gene in the liver[18]. In addition, *Cygb* is also known to act as a tumor suppressor gene[19-21] and is involved in protective mechanisms against cellular stresses such as cell injury, DNA damage, and hypoxia[16, 19, 22-25]**.** CYGB is induced by hypoxia inducible factor-1α **(**HIF-1α**)**, nuclear factor kappa-light chain enhancer of activated B cells **(**NF-κB**)**, and other inflammation-related transcription factors[26]**.** Overexpression (OE) of CYGB in lung cancer cells impaired transmigration and anchorage-independent growth under normoxic conditions but promoted these abilities under hypoxic conditions[22]. In this study, the LM8 sublines with differential abilities to metastasize to the lungs were isolated and molecular genetic analyses of these sublines revealed that LEF1-induced CYGB plays a crucial role in the extravasation step during lung metastasis**.**

2-2. Materials and methods

2-2-1. Cell culture

Murine osteosarcoma LM8 sublines, LM8-H, LM8-L and LM8-H/*Lef1*-KO were established in Kondoh laboratory[27]. These sublines were cultured in Dulbecco's Modified Eagle Medium (DMEM) supplement with 5% fetal bovine serum (FBS), penicillin (100 U/mL) and streptomycin (100 μg/mL at 37°C, 5% CO_2). Murine vascular endothelia bEnd.3 cells were purchased from ATCC (ATCC, Virginia, USA). bEnd.3 was cultured with DMEM supplemented with 10% FBS, penicillin (100 U/mL) and streptomycin (100 μg/mL at 37°C, 5% CO_2).

2-2-2. Genome-wide meta-analysis

Microarray data sets were collected from NCBI public database (http://www.ncbi.nlm.nih.gov/gds). The first data set included low and high-metastatic clinical samples of osteosarcoma (GSE21257). The second one included low- and high-metastatic cell lines of human osteosarcoma (GSE49003). To extract commonly upregulated genes in high metastatic sublines between these data sets, the data sets were analyzed using Geo2r web software on NCBI website. Then, gene ID of extracted genes based on p-value score (<0.05) was converted to murine gene ID by BioMart web software[28]. Furthermore, overlapping genes between these genes and upregulated genes in metastatic LM8 sublines were collected for further analyze.

2-2-3. qPCR and RT-PCR

Total RNA from LM8 cell line was extracted using RNeasy mini kit (Qiagen, California, USA). After RNA extraction, total RNA was converted to complementary DNA (cDNA) using Revertra Ace kit (Toyobo, Tokyo, Japan). Then, cDNA was used for qualitative PCR (qPCR) and RT-PCR. qPCR was performed using Thunderbird SYBR qPCR Mix (Toyobo). RT-PCR was performed using EmeraldAmp GT PCR Master Mix (Takara, Tokyo, Japan). The primer sets for qPCR and RT-PCR are shown in Table 2-3. For RT-

PCR, cycle number of extension step was optimized for each gene and program shown in Table 2-4 and Table 2-5 was used.

Table 2-3. Primers for qPCR and RT-PCR

Gene	Forward primer	Reverse primer
Ablim1	TACATCAGCAAGGATGGCTC	ATAATGCTTGTCGCCTGCCT
Akap12	AAGACGTGAGTTGCTCATTGT	AATCATTGGACGGCTCTGCT
Arhgef19	CCATCCGGGAAGGGAAACTG	CCACCGTGGACCTCGTTTAG
Bcar3	CTGCCAATAGGCTGCAAGCTG	AGTGCTGGACTCAGAGTGGG
Camk2n1	CAGCCCGCCACTCTTCTTAT	AACCGTTTTGTCCGAACTGC
Cygb	ACTTTAAGATTCTCTCTGGGGTC	GGTCACGTGGCTGTAGATGA
Efcab4a	AGCAAACCCAAAGAGATGTGG	TCTCGAAGCCTCAGATTCAGC
Errfi1	CCTAACAACTGTTGGATGTGCTG	TTGATCCTCTTCACGCTGTCC
Gda	TGTACATCCAGAGCCATATAAGTGA	AAAGGTAGCAGCCATGTGCC
Itpr3	TCCTGTCTAAGCTCATCCGTC	GTCCCCGAACTTGCTCTTCT
Jam2	AGTACTAGTGGCTCCTGCTGT	ATGTACTCCGGAGCTGGGTT
Mlph	AGGCATCCCGATCTTTCTTCC	TGGCTGCTGGGAGAATACTT
Pitpnc1	TGAGTGGTACGATATGACAATGGA	AGTGGAGGAGTGCTGATTGC
Prex1	TTAACAGGCTGCTGTCAACCA	CTTTCTTGATGCCGCTGTGG
RIG-I	TCACATTTGCGGAAATACAACG	GTAAGCTCTCGCTCGGTCTC
Sema3f	CCGTCGCGCACAGGATTA	CACTCCTGCATAGAGTTCCTCA
Sh3kbp1	CCCGTCGAAAAGACAATTGGG	TGGTCTTTGTCCTGCTGTCC
Synj2	TGAGTCCGAAGGGGATGTTC	TCAAGGAGCTCATGGTGTCG
Tm4sf1	GCGATGCTCGATGCTTTCTTC	CATACTCCATGGGCATCGCT

Table 2-4. Temperature condition for RT-PCR

Step	Temperature (ºC)	Time (Second)
Denaturation	98	30
Annealing	58	30
Extension	72	15

Table 2-5. Temperature condition for PCR

Step	Temperature (ºC)	Time (Second)
Pre-denaturation	94	120
Denaturation	98	10
Annealing	58	30
Extension	68	60/kb

2-2-4. Western blotting

Cell lysates were prepared with radioimmunoprecipitation assay buffer and subjected to western blot analysis using a rabbit anti-CYGB polyclonal Ab (Thermo Fisher Scientific) and a mouse anti-β-actin monoclonal Ab (Sigma Aldrich, Missouri, USA).

2-2-5. Cell proliferation assay

Cell proliferation was evaluated with the water-soluble tetrazolium salt 1 (WST-1) reagent (Roche Diagnostics, Basel, Switzerland), according to the manufacturer's instructions. Briefly, cells (1×10^3 cells/100 μL culture medium) were seeded in a 96-well plate. After culturing for 24, 48, or 72 h, the medium was removed and 100 μL WST-1 (10-fold dilution with culture medium) was added to each well. The cells were further incubated for 3 h and then the absorbance of each well was measured at 450 nm with a reference wavelength of 750 nm, after shaking the plate for 1 min with a 680XR microplate reader Model (Bio-Rad, California, USA).

2-3. Results

2-3-1. Gene screening by a genome-wide meta-analysis

To identify genes that are regulated by LEF1 and are responsible for the differential extravasation abilities among the LM8 sublines, pro-metastatic genes downstream of *Lef1* were first selected by genome-wide meta-analysis and DNA microarray data for the LM8 sublines. By performing genome-wide meta-analysis with public data sets for human OS cells, 1,912 genes were selected as upregulated genes detected in patients with highly metastatic OS. From the DNA microarray data for the LM8-L, LM8-H, and LM8-H/*Lef*1-KO sublines, 737 genes were selected as upregulated genes in correlation with the metastatic phenotype of the LM8 sublines. The genes selected by the genome-wide meta-analysis and the DNA microarray data were compared and 21 overlapping genes were extracted. Several of the candidate genes encode cell adhesion- and cell movement-related molecules (Table 2-6). Then, 13 out of 21 genes were selected based on their correlation with patient prognosis using the PROGgene database[29] (Figure 2-11 and Figure 2-12).

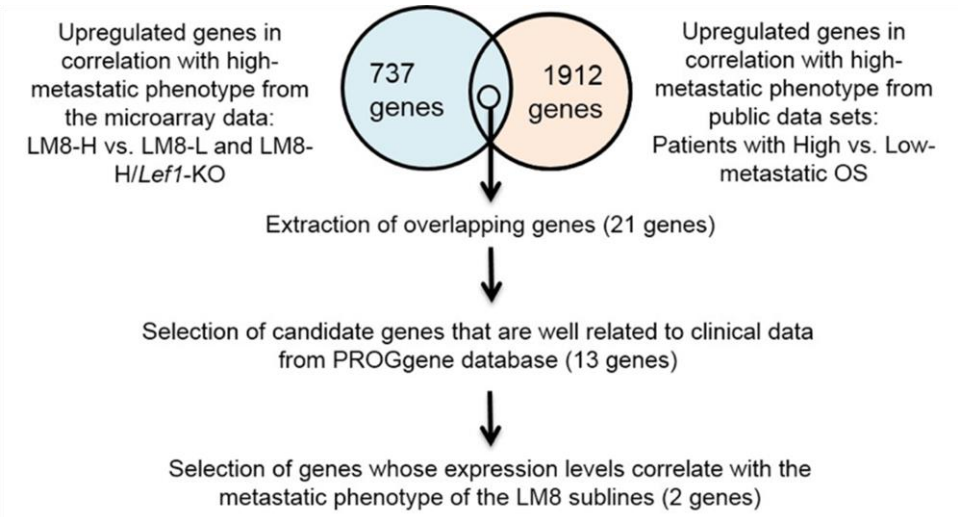

Figure 2-11. Diagram of the process used to narrow down candidate genes by genome-wide meta-analysis. The number of gene indicated for each step is number of selected genes.

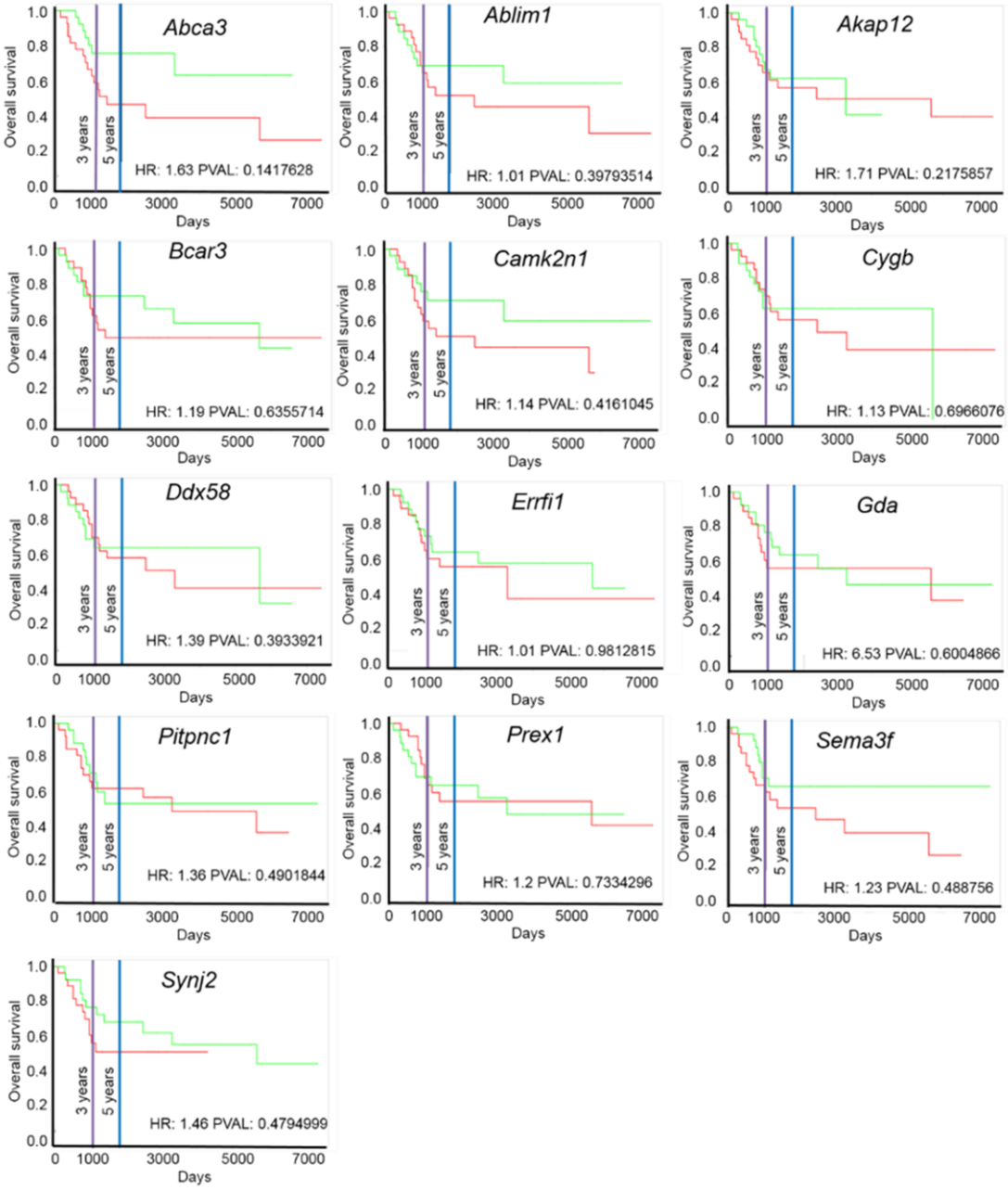

Figure 2-12. Prognostic analysis of the gene-expression levels in OS patients. The survival probabilities of patients with high- or low- expression levels of indicated genes are displayed red and green lines, respectively. HR, hazard ratio; PVAL, P-value. The genes whose expression significantly affect the patient's prognosis (HR > 1) were selected.

Table 2-6 Candidate genes selected by global gene expression analysis

Gene name	Encoded protein function
ATP binding cassette cub family a member 3 (*Abca3*) Calcium release activated channel regulator 2B (*Efcab4a*) ERBB receptor feedback inhibitor 1 (*Errfi1*) Junctional adhesion molecule 2 (*Jam2*) Leucine rich repeats and immunoglobulin like domains 1 (*Lrig1*) Ninein-like protein (*Ninl*)	Cell receptor/ transporter
Adherents junctions associated protein 1 (*Ajap1*)	Cell junction/ adhesion molecule
A-kinase anchoring protein 12 (*Akap12*) Calmodulin dependent protein kinase II inhibitor 1 (*Camk2n1*)	Protein kinase binding protein
Cytoglobin (*Cygb*) Retinoic acid-inducible gene I protein (*Ddx58*)	Oxidative stress response factor
Phosphatidylinositol-3,4,5-trisphosphate dependent rac exchange factor 1 (*Prex1*) Rho guanine nucleotide exchange factor 19 (*Arhgef19*) Guanine nucleotide-binding protein (*Gbp2*) DAB2 interactive protein (*Dap2ip*)	Small GTP-binding protein-related factor
Guanine deaminase (*Gda*)	Guanine deaminase
Phosphotriesterase related protein (*Pter*)	Phosphotriesterase
Actin binding LIM protein 1 (*Ablim1*) Cytoplasmic FMR1 interacting protein 2 (*Cyfip2*) Melanophilin (*Mlph*)	Cell movement regulator
SWI/SNF related, matrix associated, actin dependent regulator of chromatin, subfamily a, member 2 (*Smarca2*)	DNA binding protein

Expression levels of the 13 candidate genes were analyzed by reverse transcriptase-polymerase chain reaction (RT-PCR) to examine their correlations with the metastatic phenotype of the LM8 sublines (Figure 2-13). Among them, the expression levels of *Cygb* and *Ddx58* were well correlated with the metastatic phenotype of the LM8 sublines: Their expression levels are high in LM8-H cells, and low in LM8-L and LM8-H/*lef1* KO cells. Their expression levels were confirmed by qualitative PCR (qPCR) (Figure 2-14).

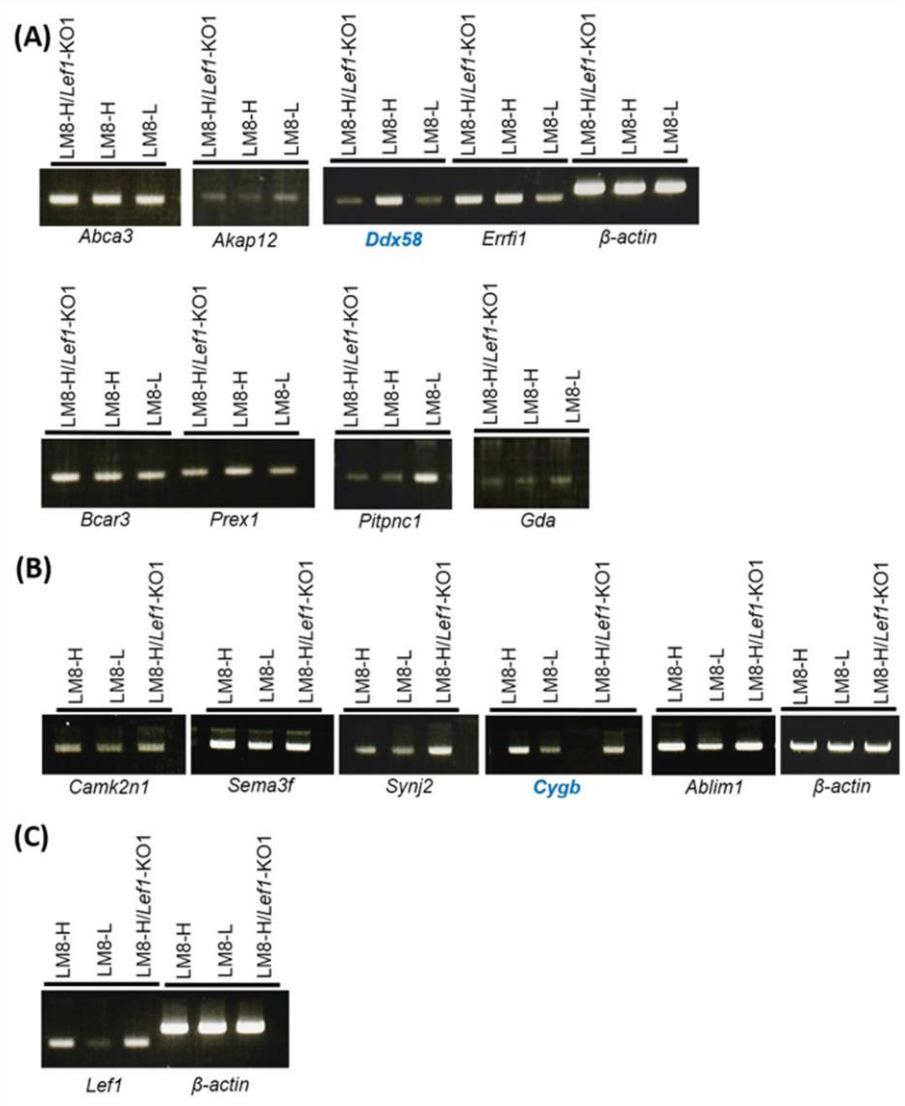

Figure 2-13. Expression levels of candidate genes in the LM8 sublines**.** Total RNA was extracted from LM8-L, LM8-H and LM8-H/*Lef1*-KO1cells and RT-PCR were performed. (**A)** Thirty cycles of PCR was performed to amplify the candidate genes, and 25 cycles were used to amplify *β-actin* gene. (**B)** Twenty-five cycles of PCR were performed to amplify *Camk2n1*, *Sema3f* and *β-actin* and 30 cycles were used for the rest of the candidate genes. (**C)** Thirty cycles of PCR were performed to amplify the *Lef1* gene, and 25 cycles were used for *β-actin*. The transcript level of *Lef1* did not change in LM8-H/*Lef1*-KO1 cells after knockout of *Lef1* using CRISPR-Cas9 system, but LEF1 protein was not detected in them.

The protein expression level of CYGB was sufficiently correlated with the metastatic phenotype of the LM8 sublines: CYGB was highly expressed in LM8-H cells but not in LM8-L and LM8-H/*lef1* KO cells (Figure 2-15). For subsequent studies, I analyzed *Cygb* because the function of *Cygb* in metastasis has not been described yet, while *Ddx58* has been reported to promote lung metastasis in several types of cancer[30, 31].

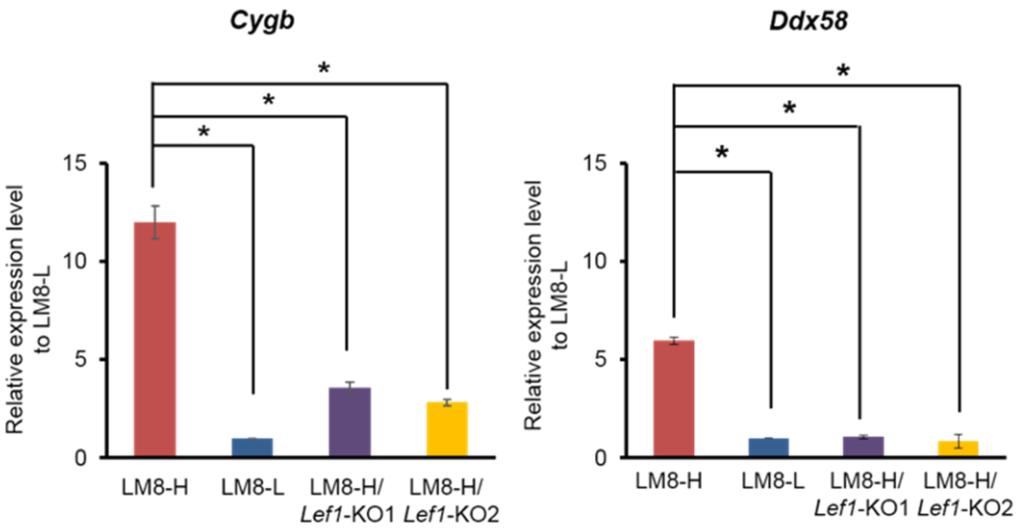

Figure 2-14. Relative *Cygb* and *Ddx58* mRNA-expression levels in the LM8 sublines to LM8-L analyzed by qRT-PCR.

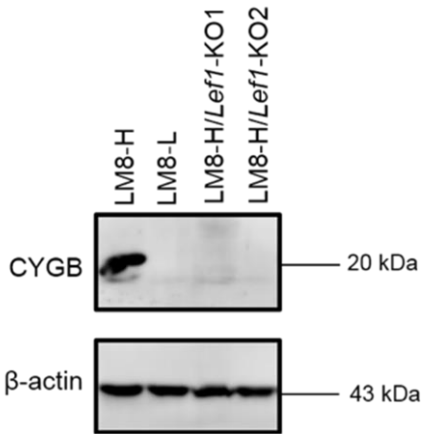

Figure 2-15. Protein-expression levels of CYGB in the LM8 sublines.

2-3-2. Establishment of CYGB overexpressing and *Cygb* knock out cell line.

To further assess the correlation between the CYGB-expression level and the extravasation ability of the LM8 sublines, Stably CYGB-overexpressing LM8-L (LM8-L/CYGB-OE) clone and two independent *Cygb*-KO LM8-H (LM8-H/*Cygb*-KO1 and LM8-H/*Cygb*-KO2) clones using two gRNAs were established (Figure 2-16A). KO of *Cygb* increased the cell-proliferation rate compared to LM8-H cells and LM8-L/CYGB-OE decreased it (Figure 2-16B). These results are consistent with the previous results showing that *Lef1*-KO increased the proliferation rate of LM8-H cells, suggesting that CYGB is a downstream effector of LEF1.

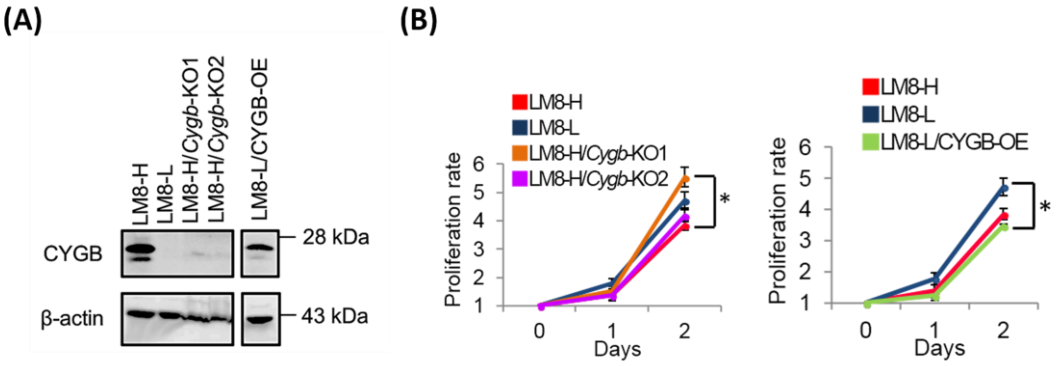

Figure 2-16. Characterization of LM8-L/CYGB OE and LM8-H/*Cygb*-KO. **(A)** Protein-expression levels of CYGB in LM8-H/*Cygb*-KO and LM8-L/CYGB-OE cells. **(B)** Cell-proliferation rates of the LM8 sublines.

Discussion

Among the 737 genes that were differentially expressed between LM8-L and LM8-H cells, 21 overlapping genes were extracted after comparing the genes selected by the genome-wide meta-analysis and the DNA microarray data. Thirteen out of 21 genes are correlated well with cancer prognosis in patients with OS and most of them have been previously reported to be associated with malignant progression, suggesting that the selection process was conducted properly. Genome analysis of transcription factor binding sites was performed using several databases[32–36]. The result reveals that *Cygb* has potential LEF1 binding sites in the promoter region (Figure 2-17), suggesting that LEF1 may directly regulate *Cygb* expression. In addition, there are some similarities between *Lef*-1-KO and *Cygb*-KO of LM8-H: the proliferation rate of LM8-H/*Cygb*-KO cells was similar to that of LM8-H/*Lef1*-KO and higher than that of LM8-H cells (Figure 2.16B), suggesting that *Cygb* is a downstream effector of LEF1 in proliferation regulation. However, regulation of *Cygb* by LEF1 is not elucidated. Since CYGB is known to be induced by HIF-1α, NF-κB, and other inflammation-related transcription factors[26], the interaction of LEF1 with these transcription factors may be important for regulating *Cygb* expression. Chromosome immuno-precipitation sequencing (ChiP-Seq) will be investigated in the future to explore interaction between LEF1 and *Cygb*.

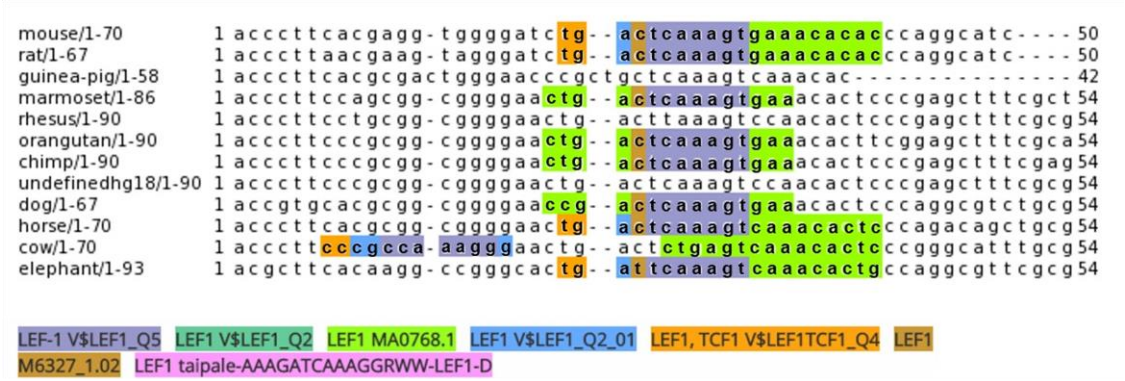

Figure 2-17. Predicted LEF1 binding site in the *Cygb* promoter region of vertebrates. Colored nucleotide sequences represent results predicted from the databases shown in the corresponding colors listed underneath.

References

1. Asai T, Ueda T, Itoh K, et al. Establishment and characterization of a murine osteosarcoma cell line (LM8) with high metastatic potential to the lung. *Int J Cancer* 1998; 76: 418–422.
2. Kha NT. Identification of genes responsible for lung metastasis of osteosarcoma by using in vivo image-guided screening system. Master thesis. Graduate School of Bioscience and Biotechnology, Tokyo Institute of Technology, 2014.
3. Thompson JR, Attia J, Minelli C. The meta-analysis of genome-wide association studies. *Brief Bioinform* 2011; 12: 259–269.
4. Evangelou E, Ioannidis JPA. Meta-analysis methods for genome-wide association studies and beyond. *Nat Rev Genet* 2013; 14: 379–389.
5. Zeggini E, Ioannidis JPA. Europe PMC Funders Group Meta-analysis in genome-wide association studies. *Pharmacogenomics* 2009; 10: 191–201.
6. Barrett JC, Clayton DG, Concannon P, Akolkar B, Cooper JD, Erlich HA *et al.* Genome-wide association study and meta-analysis find that over 40 loci affect risk of type 1 diabetes. *Nat Genet* 2009; 41: 703–707.
7. Cammen KM, Wilcox LA, Rosel PE, Wells RS, Read A. From genome-wide to candidate gene: an investigation of variation at the major histocompatibility complex in common bottlenose dolphins exposed to harmful algal blooms. *Immunogenetics* 2014; 6: 125–133.
8. Leiherer A, Muendlein A, Rein P, Saely CH, Kin z E, Vonbank A *et al.* Genome-Wide Association Study Reveals a Polymorphism in the Podocyte Receptor RANK for the Decline of Renal Function in Coronary Patients. *PLoS One* 2014; 9: 1–13.
9. Whiffin N, Hosking FJ, Farrington SM, Palles C, Dobbins SE, Zgaga L *et al.* Identification of susceptibility loci for colorectal cancer in a genome-wide meta-analysis. *Hum Mol Genet* 2014; 23: 4729–4737.
10. Amin Al Olama A, Kote-Jarai Z, Schumacher FR, Wiklund F, Berndt SI, Benlloch S *et al.* A meta-analysis of genome-wide association studies to identify prostate cancer susceptibility loci associated with aggressive and non-aggressive disease. *Hum Mol Genet* 2013; 22: 408–415.
11. Giese K, Amsterdam A, Grosschedl R. DNA-binding properties of the HMG

domain of the lymphoid-specific transcriptional regulator LEF-1. *Genes Dev* 1991; 5: 2567–2578.

12. Bruhn L, Munnerlyn A, Grosschedl R. ALY, a context-dependent coactivator of LEF-1 and AML-1, is required for TCRalpha enhancer function. *Genes Dev* 1997; 11: 640–653.
13. Hsu SC, Galceran J, Grosschedl R. Modulation of transcriptional regulation by LEF-1 in response to Wnt-1 signaling and association with beta-catenin. *Mol Cell Biol* 1998; 18: 4807–4818.
14. Nguyen DX, Chiang AC, Zhang XHF, Kim JY, Kris MG, Gerald WL *et al.* WNT/TCF signaling through LEF1 and HOXB9 mediates lung adenocarcinoma metastasis. *Cell* 2010; 138: 51–62.
15. Xu M, Jin H, Xu C-XX, Bi W-ZZ, Wang Y. MiR-34c inhibits osteosarcoma metastasis and chemoresistance. *Med Oncol* 2014; 31: 972–979.
16. Burmester T, Ebner B, Weich B, Hankeln T. Cytoglobin: a novel globin type ubiquitously expressed in vertebrate tissues. *Mol Biol Evol* 2002; 19: 416–21.
17. Burmester T, Haberkamp M, Mitz S, Roesner A, Schmidt M, Ebner B *et al.* Neuroglobin and Cytoglobin: Genes, Proteins and Evolution. *IUBMB Life* 2004; 56: 703–707.
18. Kawada N, Kristensen DB, Asahina K, Nakatani K, Minamiyama Y, Seki S *et al.* Characterization of a Stellate Cell Activation-associated Protein (STAP) with Peroxidase Activity Found in Rat Hepatic Stellate Cells. *J Biol Chem* 2001; 276: 25318–25323.
19. John R, Chand V, Chakraborty S, Jaiswal N, Nag A. DNA damage induced activation of Cygb stabilizes p53 and mediates G1 arrest. *DNA Repair (Amst)* 2014; 24: 107–112.
20. Xu H-W, Huang Y-J, Xie Z-Y, Lin L, Guo Y-C, Zhuang Z-R *et al.* The expression of cytoglobin as a prognostic factor in gliomas: a retrospective analysis of 88 patients. *BMC Cancer* 2013; 13: 1–9.
21. Thuy LTT, Matsumoto Y, Thuy TT Van, Hai H, Suoh M, Urahara Y *et al.* Cytoglobin Deficiency Promotes Liver Cancer Development from Hepatosteatosis through Activation of the Oxidative Stress Pathway. *Am J Pathol* 2015; 185: 1045–1060.

22. Oleksiewicz U, Liloglou T, Tasopoulou K-M, Daskoulidou N, Bryan J, Gosney JR *et al.* Cytoglobin has bimodal: tumour suppressor and oncogene functions in lung cancer cell lines. *Hum Mol Genet* 2013; 22: 3207–3217.
23. Yu X, Gao D. Overexpression of cytoglobin gene inhibits hypoxic injury to SH-SY5Y neuroblastoma cells. *Neural Regen Res* 2013; 8: 2198–2203.
24. Tian S-F, Yang H-H, Xiao D-P, Huang Y-J, He G-Y, Ma H-R *et al.* Mechanisms of Neuroprotection from Hypoxia-Ischemia (HI) Brain Injury by Up-regulation of Cytoglobin (CYGB) in a Neonatal Rat Model. *J Biol Chem* 2013; 288: 15988–16003.
25. Tanaka F, Tominaga K, Sasaki E, Sogawa M, Yamagami H, Tanigawa T *et al.* Cytoglobin May Be Involved in the Healing Process of Gastric Mucosal Injuries in the Late Phase Without Angiogenesis. *Dig Dis Sci* 2013; 58: 1198–1206.
26. Fordel E, Geuens E, Dewilde S, De Coen W, Moens L. Hypoxia/Ischemia and the Regulation of Neuroglobin and Cytoglobin Expression. *IUBMB Life* 2004; 56: 681–687.
27. Kha NT. Identification of Genes Responsible for Lung Metastasis of Osteosarcoma by using In Vivo Image-Guided Screening System. Tokyo Institute of Technology. 2014.
28. Smedley D, Haider S, Durinck S, Pandini L, Provero P, Allen J *et al.* The BioMart community portal: an innovative alternative to large, centralized data repositories. *Nucleic Acids Res* 2015; 43: W589–W598.
29. Goswami C, Nakshatri H. PROGgeneV2: enhancements on the existing database. *BMC Cancer* 2014; 14: 970–975.
30. Chang Y-C, Chi L-H, Chang W-M, Su C-Y, Lin Y-F, Chen C-L *et al.* Glucose transporter 4 promotes head and neck squamous cell carcinoma metastasis through the TRIM24-DDX58 axis. *J Hematol Oncol* 2017; 10: 1–12.
31. Ghildiyal R, Sen E. CK2 induced RIG-I drives metabolic adaptations in IFNγ-treated glioma cells. *Cytokine* 2017; 89: 219–228.
32. Kreft L, Soete A, Hulpiau P, Botzki A, Saeys Y, De Bleser P. ConTra v3: A tool to identify transcription factor binding sites across species, update 2017. *Nucleic Acids Res* 2017; 45: W490–W494.
33. Matys V, Kel-Margoulis O V, Fricke E, Liebich I, Land S, Barre-Dirrie A *et al.*

TRANSFAC® and its module TRANSCompel®: transcriptional gene regulation in eukaryotes. *Nucleic Acids Res* 2006; 34: D108–D110.

34. Portales-Casamar E, Thongjuea S, Kwon AT, Arenillas D, Zhao X, Valen E *et al.* JASPAR 2010: the greatly expanded open-access database of transcription factor binding profiles. *Nucleic Acids Res* 2010; 38: D105–D110.
35. Weirauch MT, Yang A, Albu M, Cote AG, Montenegro-Montero A, Drewe P *et al.* Determination and Inference of Eukaryotic Transcription Factor Sequence Specificity. *Cell* 2014; 158: 1431–1443.
36. Jolma A, Yan J, Whitington T, Toivonen J, Nitta KR, Rastas P *et al.* DNA-Binding Specificities of Human Transcription Factors. *Cell* 2018; 152: 327–339.

Chapter 3
Analysis of function of CYGB in the extravasation of the LM8 sublines

Abstract

In chapter 2, CYGB was identified as a downstream effector of transcription factor LEF1. However, functions of CYGB in extravasation ability of the LM8 sublines is unknown. To assess functions of CYGB in extravasation ability, LM8 sublines stably overexpressing CYGB or knocked out *Cygb* were established. CYGB overexpression in LM8-L subline increased the extravasation ability, whereas knocking out the *Cygb* gene in LM8-H cells reduced this ability. These results demonstrate that CYGB is important for extravasation ability of the LM8 sublines. Details molecular mechanism of CYGB on lung metastasis of the LM8 sublines were investigated based on the known function of CYGB such as regulation of nitric oxide (NO) level and arachidonic acid (AA) productions. The results suggest that CYGB promotes extravasation ability of the LM8 sublines by functions than those related to NO regulation and AA production.

3-1. Introduction

3-1-1. Characterization of metastatic phenotypes in the LM8 sublines

LM8-H and LM-L show different morphology. LM8-H has spindle shape like while LM8-L has round shape with lamellipodia. During EMT, morphology changes from round or epithelial like shaped to spindle shaped are observed in the process of cancer progression. More aggressive cancer cells assume a spindled shape[1]. Thus, LM8-H that has more aggressive behaviors with spindle shaped cell possibly exhibit EMT phenotypes (Figure 3-1). However, the expression levels of genes related to EMT of the LM8 sublines did not show typical expression patterns of epithelial or mesenchymal cells (Table 3-1). In addition, cell migration and invasion abilities were not significantly different between LM8 sublines (Figure 3-2).

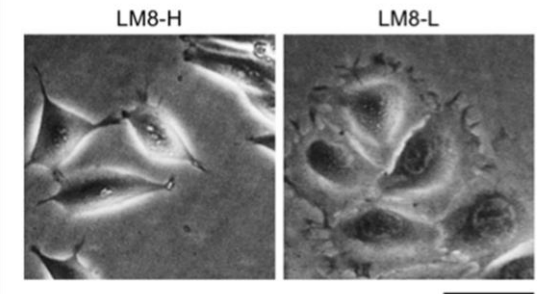

Figure 3-1. Morphology of high-metastatic (LM8-H) and low-metastatic (LM8-L) cells.

Table 3-1. Expression level of EMT-related genes from LM8 microarray data.

Gene name	Expression level		Up/down regulated in LM8-H (vs LM8-L)
	LM8-H	LM8-L	
Mesenchymal marker			
Wnt Family Member 5A (*Wnt5a*)	0.02	0.04	down
Transforming Growth Factor Beta 1 (*Tgfb1*)	3.6	2.1	Up (<2 folds)
Insulin Like Growth Factor 1 (*Igf1*)	0.22	0.91	down
Snail Family Transcriptional Repressor 1 (*Snai1*)	2.5	7.7	down
Vimentin (*Vim*)	123	135	down
Fibronectin 1 (*Fn1*)	37.15	31.44	Up (<2 folds)
Cadherin 1 (*Cdh1*)	0.02	0.02	equal
Integrin Subunit Beta 1 (*Itgb1*)	3.24	3.91	down
Runt Related Transcription Factor 3 (*Runx3*)	0.62	1.28	down
Neuropilin 2 (*Nrp2*)	10.01	9.45	Up (<2 folds)
Raf-1 Proto-Oncogene (*Raf1*)	31.98	36.32	down
B-Cell CLL/Lymphoma 2 (*Bcl2*)	1.51	3.09	down
SRY-Box 9 (*Sox9*)	1.25	2.28	down
Mitogen-Activated Protein Kinase Kinase 1 (*Map2k1*)	5.81	9	down
Matrix Metallopeptidase 2 (*Mmp2*)	1.56	1.5	equal
Matrix Metallopeptidase 9 (*Mmp9*)	0.43	0.04	Up
Epithelial marker			
Syndecan 1 (*Sdc1*)	7.69	4.09	Up (<2 folds)
Syndecan 2 (*Sdc2*)	9.41	14.7	down
Cadherin 2 (*Cdh2*)	0.14	0.14	equal
Collagen, Type VIII, Alpha 2 (*Col8a2*)	0.33	0.41	down
Tight Junction Protein 1 (*Tjp1*)	7.76	4.22	Up (<2 folds)
Occludin (*Ocln*)	0.02	0.01	Up (low expression level)

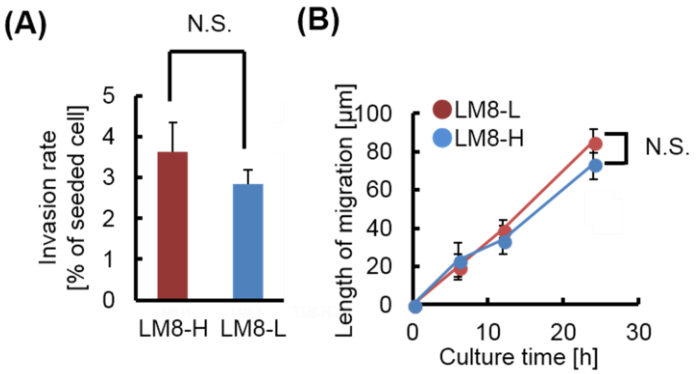

Figure 3-2. Characterization of the LM8 sublines. (A) Migration abilities of the LM8 sublines assessed by performing wound-healing assay. n = 3. (B) Invasion abilities of LM8 sublines in collagen matrix. n = 5.

3-1-2. Function of LEF1 in lung metastasis in the LM8 sublines

To search mechanism that LEF1 is involved in lung metastasis of the LM8 sublines, extravasation ability of the LM8 sublines was assessed. Extravasation ability of cancer cells can be assessed as their *in vitro* abilities to attaches to and transmigrate through endothelial cell monolayers. Thus, adhesion and transmigration assays were performed with cultured monolayers of murine endothelial cells. Adhesion and transmigration abilities were significantly decreased in LM8-L and LM8-H/*Lef1*-KO1 cells, compared to LM8-H cells (Figure 3-3 and 3-4). These results suggest that the extravasation step could be responsible for differential lung-metastasis abilities of LM8-L and LM8-H cells, and that LEF1 function is indispensable in the extravasation of LM8-H cells to the lungs.

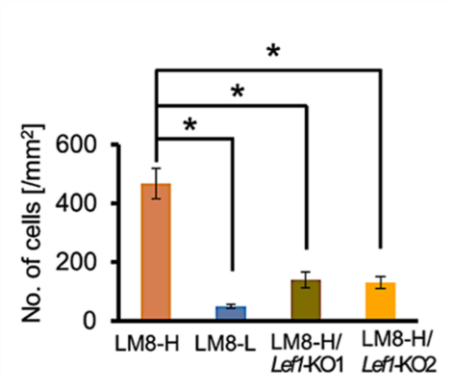

Figure 3-3. Adhesion abilities of the LM8 sublines to the endothelial monolayer. The number of fluorescently labeled cells (LM8 sublines) attached to the endothelial monolayer was counted. n = 3, **P* < 0.05. (vs. LM8-H).

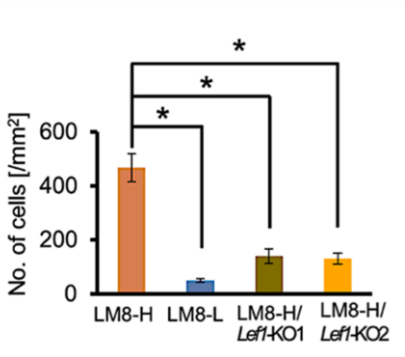

Figure 3-4. Transmigration ability of LM8 sublines into the vascular endothelial monolayer. The number of fluorescently labeled cell (for each LM8 subline) that migrated through the vascular endothelial monolayer was counted. n = 3, **P* < 0.05 (vs. LM8-H).

3-1-3. Function of CYGB on lipid oxidation

Recently, function of CYGB on lipid oxidation was discovered. CYGB converts several types of phospholipids such as phosphatidylinositol (3,4,5)-trisphosphate (an important signal mediator of the AKT signaling pathway) to arachidonyl-containing lipid. Arachidonyl-containing lipid can be converted to AA by phospholipase enzymes[2]. AA increases the migratory activity of cancer cells through activation of RhoA and RhoC[3]. Activation of RhoA and RhoC increased actin remodeling in the cell through many effectors including cofilin and kinectin[4]. Moreover, AA promoted cancer progression and metastasis in several types of cancer thorugh different pathways such as PI3K/AKT and p38/ERK[5, 6]. Therefore, CYGB may promote metastasis by increasing AA content in the LM8 sublines.

3-1-4. Role of NO in cancer progression

NO is a major signaling molecule related to inflammation pathway and vascular relaxation generated by the action of nitric oxide synthases (NOS)[7]. Previous studies indicated that NO displayed pro- and anti-tumor effects depended on concentration manner[8]. Low concentration (<100 nM) of NO promoted cellular proliferation and angiogenesis. Medium concentration (100-500 nM) also accelerated malignant

phenotypes including invasiveness and metastasis. On the other hand, high concentration (>500 nM) induced DNA damage and apoptosis[8]. Previous studies have described that CYGB is involved in regulation of NO level in the cell by scavenge NO[9, 10]. CYGB binds to oxygen and transfer its oxygen to convert NO to nitrate[10]. Therefore, CYGB could be an important modulator of NO concentration in cancer cells and may regulate malignancy of cancer cells. Therefore, molecular crosstalk between NO and CYGB may contribute to CYGB-mediated increase in extravasation ability of the LM8 sublines.

3-2. Materials and methods

3-2-1. Cell culture

Murine osteosarcoma the LM8 sublines, LM8-H, LM8-L and LM8-H/*Lef1*-KO were established in Kondoh laboratory. These sublines were cultured in Dulbecco's Modified Eagle Medium (DMEM) supplement with 5% fetal bovine serum (FBS), penicillin (100 U/mL) and streptomycin (100 μg/mL at 37°C, 5% CO_2). Murine vascular endothelia bEnd.3 cells were purchased from ATCC (ATCC, Virginia, USA). bEnd.3 was cultured with DMEM supplemented with 10% FBS, penicillin (100 U/mL) and streptomycin (100 μg/mL at 37°C, 5% CO_2).

3-2-2. Establishment of an LM8 cell line with stable CYGB overexpression

To establish stable cell lines overexpressing *Cygb*, the sleeping beauty transposon system was employed[11-13]. The pT2/*Cygb* or pT2-MCS-SV Neo and pCMV(CAT)T7-SB100 plasmids (34879, Addgene) were co-transfected into LM8-L cells using an electroporator (Nepa Gene, Chiba, Japan) according to the manufacturer's instructions. After 48 h, the culture medium was changed to selection medium containing 1μg/mL G418 (Roche Life Sciences, Basel, Switzerland). The cells were further cultured in selection medium for 14 days and single colonies were isolated to establish CYGB-overexpressing LM8-L (CYGB-OE) cells

3-2-3. Construction of LM8-H/*Cygb*- KO subline by using CRISPR-Cas9 system

Two guide RNA (gRNA1 and gRNA2) used for editing *Lef1* and *Cygb* were constructed using CRISPR design software[14]. The sequences of gRNA1 and gRNA2 used for targeting *Lef1* are 5′-TTGTTGTACAGGCCTCCGTC-3′ and 5′-GTACGGGTCGCTGTTCATAT-3′, respectively. The sequences of gRNA1 and gRNA2 used for targeting *Cygb* are 5′-GAAGGCGGTTCAGGCTACGT-3′ and 5′-TGAAGTACTGCTTGGCCGAA-3′, respectively. The *Lef1* and *Cygb* gRNAs were inserted into a unique *Bbs*I site of the pX330 plasmid (42230, Addgene). We employed a fluorescence indicator system using the pCAG/EGxxFP plasmid[15] provided by Dr. Ikawa (Osaka University, Osaka, Japan) to select cells whose genomes were correctly edited using CRISPR-Cas9 system. GFP-positive colonies were selected and two independent LM8-H*/Lef1*-KO and LM8-H*/Cygb*-KO clones each were established from the gRNA1- and gRNA2-mediated KO cells.

3-2-4. Vector construction

The coding sequence of *Cygb* (NM_030206) was amplified using the KOD® FX Kit (Toyobo) with the following primer set: Forward, 5′-TCATGGAGAAA-GTGCCGGGCG-3′ and Reverse, 5′-CCCAAAGTGCTGCCAGGGAGG-3′. The PCR product was purified by Gelase® (Epicentre, Wisconsin, USA) and ligated into an *Eco*RV-digested pcDNA3.1-myc-His plasmid (Invitrogen, California, USA) using the Quick Ligation Kit (New England BioLabs, Massachusetts, USA) to construct the pcDNA3.1/*Cygb*. The pT2-MCS-SVNeo vector containing multi-cloning sites (MCS) was constructed using the pT2-SVNeo vector (26553, Addgene), as described previously[11]. The fragment containing the *Cygb* cording sequence was obtained by digesting pcDNA3.1/*Cygb* with *Eco*RI and *Not*I and inserting the liberated fragment into an *Eco*RI- and *Not*I-digested pT2-MCS-SVNeo plasmid.

3-2-5. Extravasation assay

Cells were labeled with 25 μM CellTracker® Green and intravenously injected into C3H mice (1×10^6 cells/100 μL PBS). DyLight® 594-labeled isolectin B4 (6 mg/kg) (Vector

Laboratories, California, USA) was intravenously injected to stain endothelial cells 5 min before dissecting mice. The lungs were removed and observed under a confocal fluorescence microscope (Carl Zeiss, Jena, Germany) 48 h after LM8 injection. The average fluorescence intensity of 3 fields/sample was quantitatively analyzed using Image J software[16] (Figure 3-5).

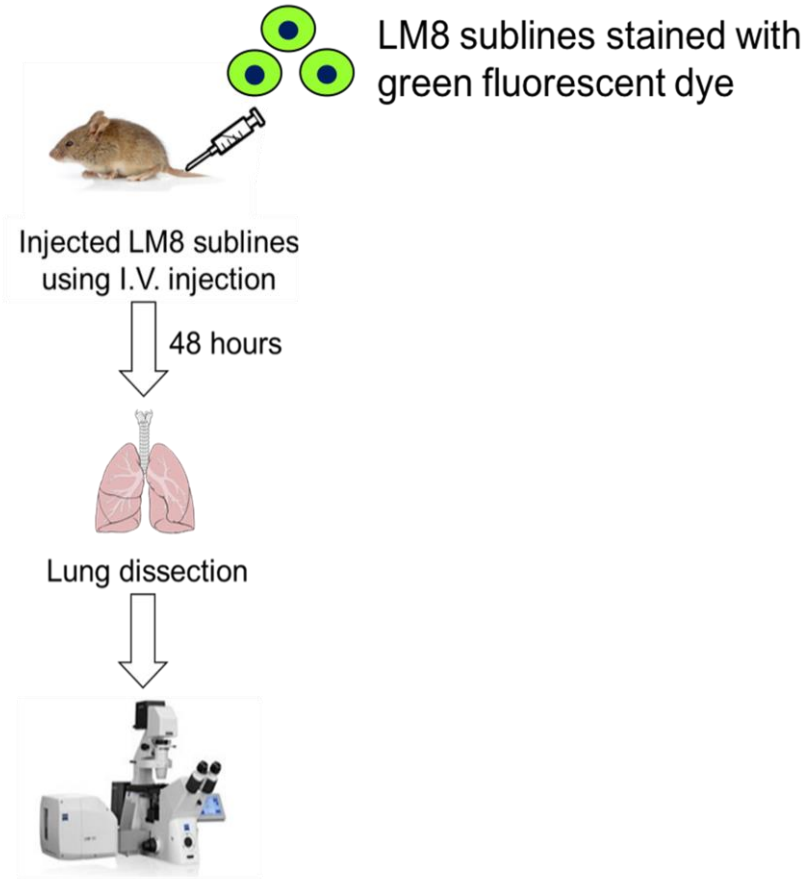

Figure 3-5. Summary diagram of extravasation assay.

3-2-6. Cell adhesion assay

bEnd.3 cells were seeded on a 24-well plate (1.0×10^5 cells/well) and cultured for 3 days. LM8 sublines were labeled with 25 μM CellTracker® Green for 30 min. After washing with PBS, LM8 cells (5×10^4) were seeded into 24-well plates with bEnd.3 monolayers. After a 1-h incubation, each well was washed 3 times with PBS. The number of LM8 cells attached to the bEnd.3 monolayer was observed by fluorescence microscopy (4 fields/well) and quantitatively analyzed using Image J software[16]. Each sample was analyzed in triplicate (Figure 3-6).

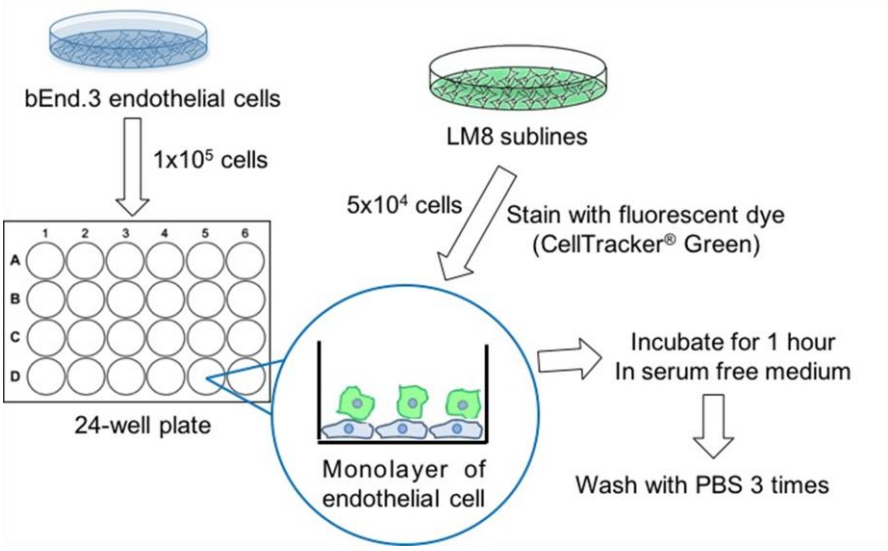

Figure 3-6. Summary diagram of adhesion assay.

3-2-7. Transmigration assay

bEnd.3 cells (1.0×10^5 cells) were seeded in the top filters with 8 μm-pore Transwell® plate (Corning, New York, USA) and grown for 3 days. The LM8 sublines were labeled with 25 μM CellTracker® Green for 30 min. After washing with PBS, the cells (5×10^4 cells) were seeded on bEnd.3 monolayers. After a 24-h incubation, the unmigrated cells were wiped off with a cotton swab, and then the filter was fixed with 4% paraformaldehyde for 20 min. Then, the migrated cells on the filter were observed under a fluorescence microscope (4 fields/filter) and the number of migrated cells was analyzed

using Image J software[16]. The results are shown as the average number of cells per field. Each sample was analyzed in triplicate (Figure 3-7).

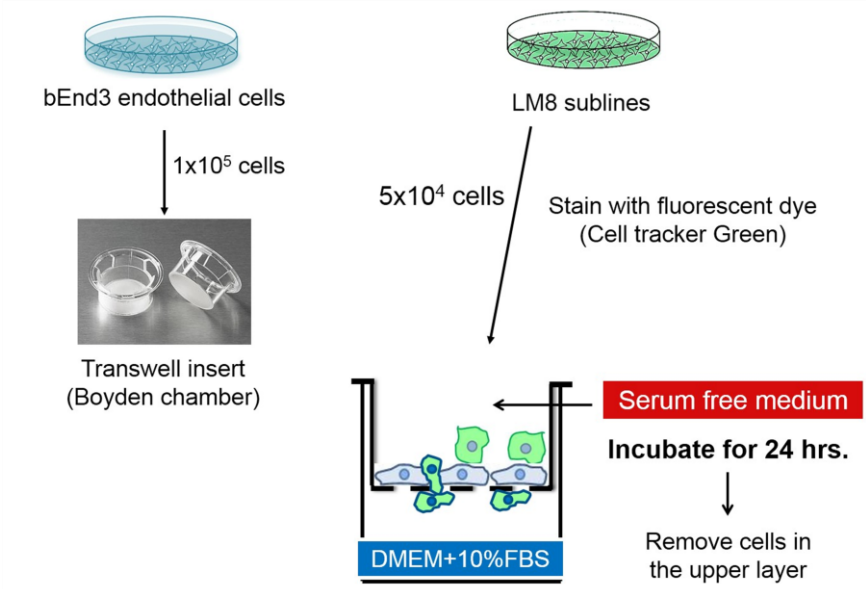

Figure 3-7. Summary diagram of transmigration assay.

3-2-8. Analysis of nitric oxide levels in the LM8 sublines

LM8 sublines (2 x 10^6 cell/well) were seeded in 24 well plate and then cultured in serum free DMEM culture medium for 24 h. Nitric oxide level was measured by using Nitric oxide assay fluorometric kit (Abcam, Cambridge, United Kingdom). The procedures were followed the manufacturer leaflet. Fluorescent intensities were measured at excitation/emission wavelengths of 360/450 nm, respectively, by using a fluorescent microplate reader (TECAN infinite F500, TECAN, Aktiengesellschaft, Switzerland). Nitric oxide level of each sample was calculated by the use of a calibration curve from standard samples.

3-2-9. Measurement of arachidonic acid

LM8 sublines were cultured with serum-free DMEM for 12 h. Then, total lipid was extracted from 2 x 10^6 cells by using chloroform and methanol. The organic solvent was evaporated and then resuspended in 200 μL methanol. Arachidonic concentration in the sample were analyzed by using liquid chromatography/mass spectroscopy LCMS-8050 (LC/MS) (Shimadzu, Kyoto, Japan) and compared with standard 20 ng arachidonic acid. Each subline was analyzed by using 3 independent samples.

3-3. Results

3-3-1. Functions of CYGB in adhesion and transmigration abilities *in vitro*

To assess effect of CYGB on extravasation ability of the LM8 sublines, adhesion and transmigration assay were performed. Adhesion and transmigration abilities were significantly higher in LM8-L/CYGB-OE cells compared to LM8-L cells (Figure 3-8). In contrast, KO of *Cygb* significantly decreased the adhesion and transmigration abilities of LM8- H cells (Figure 3-9) . These results strongly suggested that CYGB promoted extravasation with the LM8 sublines by increasing their adhesion and transmigration abilities.

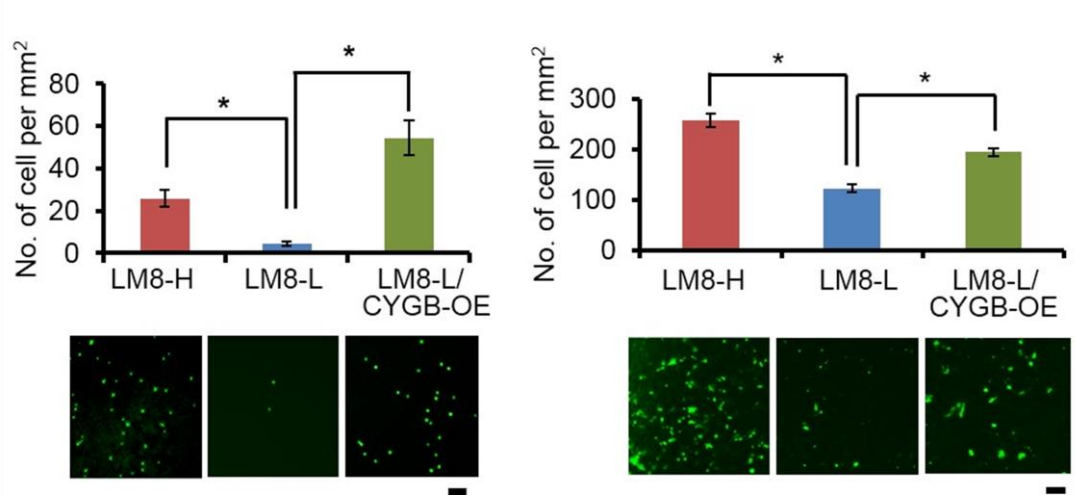

FIGURE 3-8. The adhesion and transmigration abilities of LM8-L/CYGB-OE. Cells were quantitatively analyzed (graphs) by determining the number of fluorescently labeled cells attached to (left) and transmigrating through (right) a vascular endothelial monolayer, respectively. Representative images are shown depicting the fluorecently labeled cells that were counted (photos). n = 3, $*P < 0.05$. Bars, 100 μm.

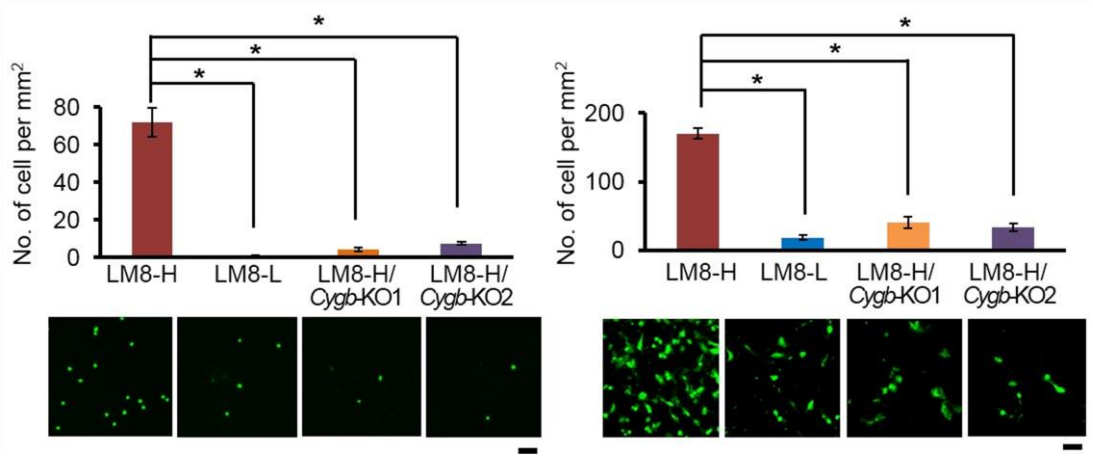

FIGURE 3-9. The adhesion and transmigration abilities of LM8-H/*Cygb*-KO. Cells were quantitatively analyzed (graphs) by determining the number of fluorescently labeled cells attached to (left) and transmigrating through (right) a vascular endothelial monolayer, respectively. Representative images are shown depicting the fluorecently labeled cells that were counted (photos). n = 3, $*P < 0.05$. Bars, 100 μm.

3-3-2. Effect of NO on CYGB function in extravasation ability of the LM8 sublines

Details mechanism of CYGB on extravasation ability of LM8 sublines was investigated. CYGB is widely known as a NO regulator and NO suppress cell adhesion molecules on the vascular endothelial cells. Thus, I hypothesized that CYGB may increase NO levels of the LM8 sublines to influence vascular endothelial cells, leading to an increase of extravasation of the LM8 sublines. Therefore, total NO levels of the LM8 sublines were measured. I found that NO level was not significantly different among the LM8 sublines (Figure 3-10A). In addition, transmigration ability of LM8-H was not affected by iNOS inhibitor treatment (Figure 3-10B). These results demonstrated that NO is not involved in the extravasation ability of the LM8 sublines.

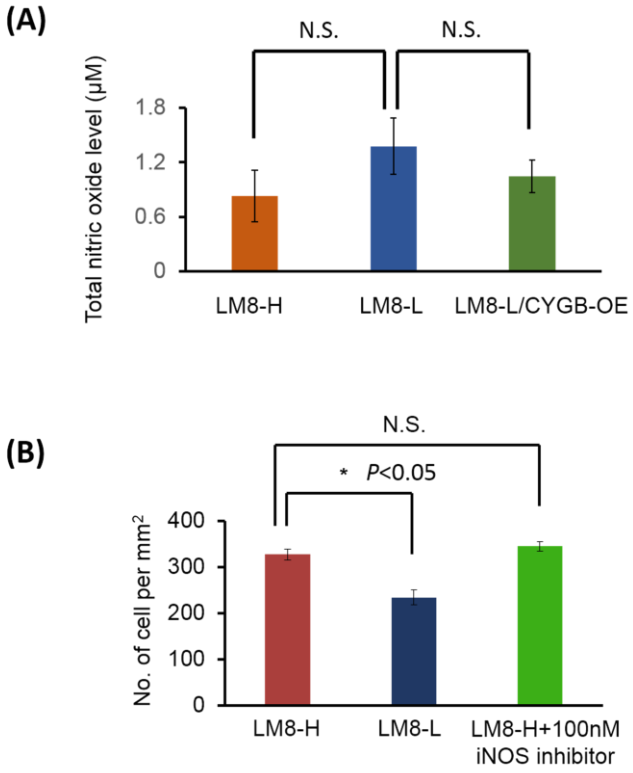

Figure 3-10. Effect of nitric oxide (NO) level on extravasation ability in LM8 sublines. **(A)** Total NO levels in the LM8 sublines. **(B)** Effect of an iNOS inhibitor on transmigration ability of LM8-H. LM8-H cell was treated with an iNOS inhibitor, aminoguanidine hydrochloride, for 24 h before transmigration assay. n=3 *P<0.05.

3-3-3. Function of CYGB at AA level in the LM8 sublines.

Recently, novel function of CYGB on phospholipid peroxidation to produce arachidonyl containing lipid, a precursor of AA[2]. AA is an important mediator for many signaling pathways that related to cancer progression including those involved in NFκB, ERK and AKT[3, 5, 6]. Therefore, I hypothesized that CYGB may affect AA levels in the LM8 sublines to influence their extravasation ability. AA level in the LM8 sublines was assessed and I found that AA levels were not significantly different between sublines (Figure 3-6). In addition, mRNA expression levels of AA downstream effectors were assessed by using microarray analysis. Three of the 21 genes correlated well with the metastatic phenotypes of the LM sublines (Table 3-2). These results suggest that AA is

not involved in the CYGB function, which increases the extravasation of the LM8 sublines.

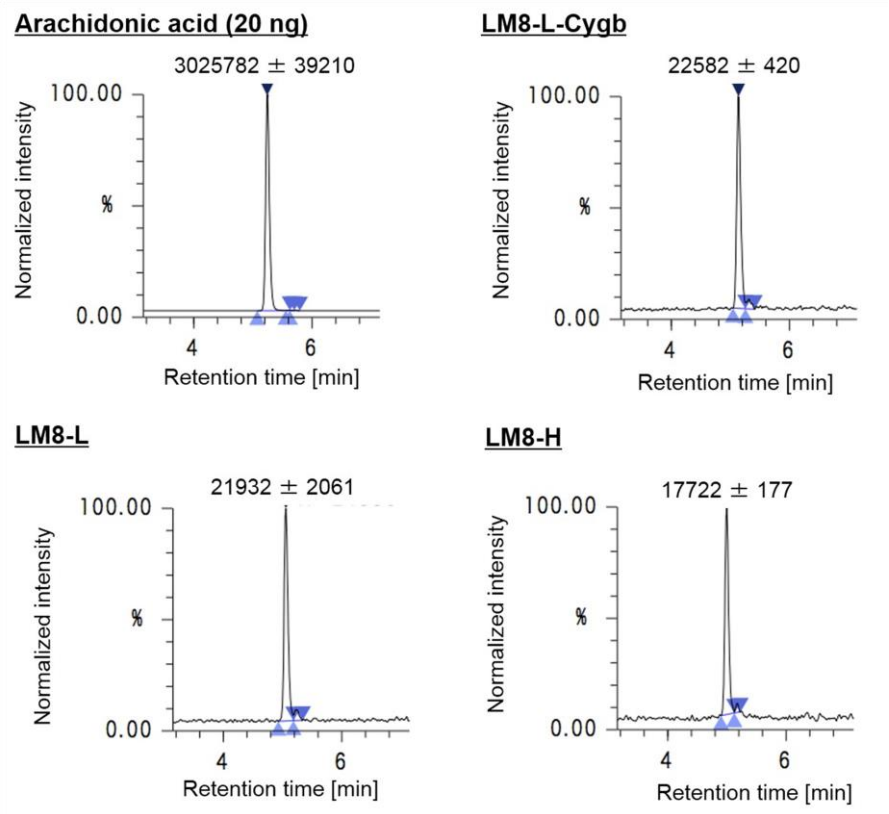

Figure 3-11. Comparison of amount of arachidonic acid in LM8 sublines. Arachidonic acid level in LM8 sublines was determined by using LC/MS. Retention time of arachidonic acid was determined with synthetic arachidonic acid (AA). Mean area of AA peak was shown in each diagram (n=3).

Table 3-2. Expression levels of AA downstream effectors.

Gene name	Expression level			Up/down regulated in LM8-H (vs LM8-L)	Up/down regulated in LM8-H/*Lef1*-KO (vs LM8-H)
	LM8-H	LM8-L	LM8-H/*Lef1*-KO		
Jun	10.58	3.78	9.55	Up	Down (less than 2 times)
Atf3	1.50	0.84	1.74	Up (less than 2 times)	Up (less than 2 times)
Fosl1	1.94	3.41	1.49	Down	Down (less than 2 times)
Fos	0.43	0.06	0.06	Up	Down
Egr1	0.29	0.05	0.01	Up	Down
Maff	0.65	0.38	0.32	Up (less than 2 times)	Down
Snai2	32.49	31.27	20.38	Equal	Down
Znhit6	27.55	23.86	31.52	Up (less than 2 times)	Up (less than 2 times)
Klf5	0.04	0.03	0.01	Up (Low expression level)	Down (Low expression level)
Ptp4a1	4.29	6.86	4.53	Down	Up (less than 2 times)
Cxcr2	0.03	0.02	0.01	Up (Low expression level)	Down (Low expression level)
Rapgef2	7.17	6.89	8.04	Equal	Up (less than 2 times)
Stc2	0.40	2.93	1.32	Down	UP
Sqstm1	8.37	7.07	9.48	Up (less than 2 times)	Up (less than 2 times)
Arhgdia	0.02	0.01	0.01	Up (Low expression level)	Down (Low expression level)
Itga6	13.00	12.06	16.05	Up (less than 2 times)	Up (less than 2 times)
Tnfrsf12a	13.01	18.68	13.98	Down	Up (less than 2 times)
Pmaip1	0.02	0.01	0.01	Equal Low expression level	Down Low expression level
Phlda1	6.70	1.85	1.45	Up	Down
Hmox1	5.60	10.99	5.85	Down	Up (less than 2 times)
Ddit4	78.83	76.86	66.36	Up (less than 2 times)	Down

Discussion

In this chapter, functions of CYGB on extravasation ability of the LM8 sublines was confirmed. I conducted two experiments to elucidate the molecular mechanism by which CYGB directly functions in promoting extravasation of the LM8 sublines based on the proposed functions of CYGB. CYGB has been suggested to act as a NO dioxygenase[7] and NO prevents endothelial activation by inhibiting the expression of adhesion molecules such as VCAM-1 and ICAM-1[17, 18]. I hypothesized that CYGB decreases NO release from LM8 cells. Since NO decreases the expression of adhesion molecules such as VCAM-1 and ICAM-1 on the vascular endothelial cells (Figure 3-12), the reduction of NO increases the interaction between cancer cell and the vascular endothelial cells through adhesion molecules. The interaction is an important step for extravasation[19] and thus the reduction of NO increase extravasation of LM8 sublines. Therefore, I first investigated whether CYGB reduces the NO levels in the LM8 sublines and promotes extravasation ability of the LM8 sublines.

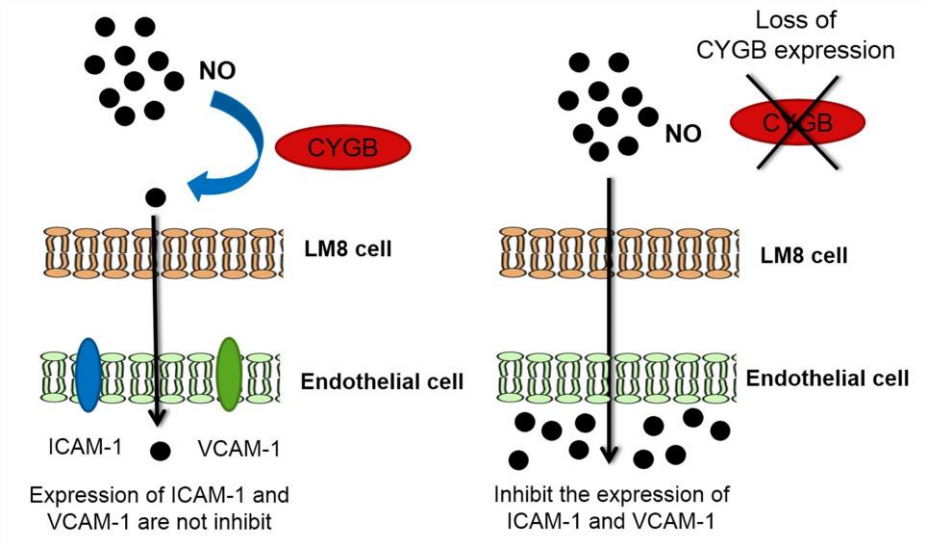

Figure 3-12. A possible mechanism for promoting the extravasation ability of LM8 sublines by CYGB.

I found only slight differences in the total NO species levels among the LM8 sublines and little influence of inhibitors of NO species on them (Figure 3-10). Although NO reduction

by CYGB may contribute to metastasis, the subtle differences in NO levels among the LM8 sublines cannot explain the significant differences in lung metastatic potential found among them, suggesting that NO may not be a major player in the CYGB-mediated extravasation.

AA increases the migratory activity of cancer cells through activation of RhoA and RhoC[3]. Furthermore, recent findings imply that CYGB functions in lipid oxidation[1]; CYGB modifies several types of phospholipids such as phosphatidylinositol (3,4,5)-trisphosphate (an important signal mediator of the AKT signaling pathway) to form arachidonyl-containing lipid. Therefore, I secondly examined the content of AA in the LM8 sublines. No difference was found in the AA contents among the LM8 sublines (Figure 3-11). In addition, expression levels of genes related to AA in LM8 sublines did not correlate well with lung metastatic phenotypes of the LM8 sublines, suggesting that AA may not function as an effector molecule of CYGB to promote the extravasation of LM8 sublines. Three genes that correlate well with lung metastatic phenotypes of the LM8 sublines are downstream effectors of Wnt signaling pathway and regulated by LEF1[20-22]. Thus, expression levels of these genes are influences by factor other than arachidonic acid, such as LEF1 in the LM8 sublines. These results suggest that the function of CYGB which has not yet been identified contributes to promotion of the extravasation.

The detailed mechanism of CYGB in cancer progression and lung metastasis is largely unknown. *Cygb* is also known to act as a tumor suppressor gene: it induced cancer cell apoptosis and suppressed cell migration[23-25]. In a certain condition such as hypoxia, CYGB promotes cancer survival by increasing cell migration and resistance to oxidative stress by decrease reactive oxygen species (ROS) and NO level in the cell[23]. These data suggest that CYGB may be involve in lung metastasis process by promoting cancer cell survival inside blood vessel and lung parenchyma. To my knowledge, the function of CYGB in metastasis, especially extravasation and cell-cell interactions in cancer, has not been reported. Further investigation of the molecular mechanism of extravasation that CYGB is involved in may provide with a new therapeutic target for preventing osteosarcoma metastasis. Further studies of the molecular mechanism of extravasation

involving CYGB may provide new therapeutic targets for preventing metastasis of osteosarcoma.

References

1. Shih J-Y, Yang P-C. The EMT regulator slug and lung carcinogenesis. *Carcinogenesis* 2011; 32: 1299–1304.
2. Tejero J, Kapralov AA, Baumgartner MP, et al. Peroxidase activation of cytoglobin by anionic phospholipids: Mechanisms and consequences. *Biochim Biophys Acta - Mol Cell Biol Lipids* 2016; 1861: 391–401.
3. Brown M, Roulson J-A, Hart CA, et al. Arachidonic acid induction of Rho-mediated transendothelial migration in prostate cancer. *Br J Cancer.* 2014; 110: 2099–2108.
4. Prudnikova TY, Rawat SJ, Chernoff J. Molecular Pathways: Targeting the Kinase Effectors of RHO-Family GTPases. *Clin Cancer Res* 2015; 21: 24 LP-29.
5. Villegas-Comonfort S, Castillo-Sanchez R, Serna-Marquez N, et al. Arachidonic acid promotes migration and invasion through a PI3K/Akt-dependent pathway in MDA-MB-231 breast cancer cells. *Prostaglandins, Leukot Essent Fat Acids* 2014; 90: 169–177.
6. Garcia MC, Ray DM, Lackford B, et al. Arachidonic Acid Stimulates Cell Adhesion through a Novel p38 MAPK-RhoA Signaling Pathway That Involves Heat Shock Protein 27. *J Biol Chem* 2009; 284: 20936–20945.
7. Gardner AM, Cook MR, Gardner PR. Nitric-oxide Dioxygenase Function of Human Cytoglobin with Cellular Reductants and in Rat Hepatocytes. *J Biol Chem* 2010; 285: 23850–23857.
8. Burke AJ, Sullivan FJ, Giles FJ, et al. The yin and yang of nitric oxide in cancer progression. *Carcinog* 2013; 34: 503–512.
9. Li H, Hemann C, Abdelghany TM, et al. Characterization of the Mechanism and Magnitude of Cytoglobin-mediated Nitrite Reduction and Nitric Oxide Generation under Anaerobic Conditions. *J Biol Chem* 2012; 287: 36623–36633.
10. Bholah TC, Neergheen-bhujun VS, Hodges NJ, et al. Cytoglobin as a Biomarker in Cancer : Potential Perspective for Diagnosis and Management. *Biomed Res Int* 2015; 2015: 1–7..

11. Cui Z, Geurts AM, Liu G, et al. Structure–function analysis of the inverted terminal repeats of the sleeping beauty transposon. *J Mol Biol.* 2002; 318: 1221–1235.
12. Aronovich EL, McIvor RS, Hackett PB. The Sleeping Beauty transposon system: a non-viral vector for gene therapy. *Hum Mol Genet.* 2011; 20: R14–R20.
13. Ivics Z, Hackett PB, Plasterk RH, et al. Molecular reconstruction of sleeping beauty, a tc1-like transposon from fish, and its transposition in human cells. *Cell.* 1997; 91: 501–510.
14. Ran FA, Hsu PD, Wright J, et al. Genome engineering using the CRISPR-Cas9 system. *Nat Protoc* 2013; 8: 2281–2308.
15. Mashiko D, Young SAM, Muto M, et al. Feasibility for a large scale mouse mutagenesis by injecting CRISPR/Cas plasmid into zygotes. *Dev Growth Differ* 2014; 56: 122–129.
16. Abràmoff MD, Magalhães PJ, Ram SJ. Image processing with imageJ. *Biophotonics Int* 2004; 11: 36–41.
17. Lee SK, Kim JH, Yang WS, et al. Exogenous Nitric Oxide Inhibits VCAM-1 Expression in Human Peritoneal Mesothelial Cells. *Nephron* 2002; 90: 447–454.
18. Khan B V, Harrison DG, Olbrych MT, et al. Nitric oxide regulates vascular cell adhesion molecule 1 gene expression and redox-sensitive transcriptional events in human vascular endothelial cells. *Proc Natl Acad Sci* 1996; 93: 9114–9119.
19. Reymond N, D'Agua BB, Ridley AJ. Crossing the endothelial barrier during metastasis. *Nat Rev Cancer* 2013; 13: 858–870.
20. Jeong W-J, Ro EJ, Choi K-Y. Interaction between Wnt/β-catenin and RAS-ERK pathways and an anti-cancer strategy via degradations of β-catenin and RAS by targeting the Wnt/β-catenin pathway. *NPJ Precis Oncol* 2018; 2: 5.
21. Yu S, Li F, Xing S, et al. Hematopoietic and Leukemic Stem Cells Have Distinct Dependence on Tcf1 and Lef1 Transcription Factors. *J Biol Chem* 2016; 291: 11148–11160.
22. Maxime B, A. CJ, Amélie O, et al. Skin tumors with matrical differentiation: lessons from hair keratins, beta-catenin and PHLDA-1 expression. *J Cutan Pathol* 2014; 41: 427–436.
23. Kelm M. Nitric oxide metabolism and breakdown. *Biochim Biophys Acta* -

Bioenerg 1999; 1411: 273–289.

24. Oleksiewicz U, Liloglou T, Field J, Xinarianos G. Cytoglobin: biochemical, functional and clinical perspective of the newest member of the globin family. *Cell Mol Life Sci* 2011; 68: 3869–3883.
25. Shivapurkar N, Stastny V, Okumura N, Girard L, Xie Y, Prinsen C *et al.* Cytoglobin, the newest member of the globin family, functions as a tumor suppressor gene. *Cancer Res* 2008; 68: 7448–7456.
26. Thuy LTT, Matsumoto Y, Thuy TT Van, Hai H, Suoh M, Urahara Y *et al.* Cytoglobin Deficiency Promotes Liver Cancer Development from Hepatosteatosis through Activation of the Oxidative Stress Pathway. *Am J Pathol* 2015; 185: 1045–1060.

Chapter 4

Functions of *Cygb* on lung-metastatic ability of the LM8 sublines *in vivo*.

Abstract

In the previous chapter, functions of CYGB on adhesion and transmigration abilities were demonstrated *in vitro*. Correlation between CYGB and extravasation ability of the cancer is largely unknown. In this chapter, functions of CYGB in lung metastasis were assessed in mouse model. Knock-out of *Cygb* in LM8-H cells significantly decreased their extravasation ability. Number and size of foci in the lung were significantly decreased at 16 days after injected cancer cell into the mouse. These results demonstrated that CYGB is a key factor to regulate lung metastasis in the LM8 sublines. The results uncovered a novel LEF1-CYGB axis in OS lung metastasis and may open a new avenue for developing therapeutic strategies to prevent OS lung metastasis.

4-1. Introduction

4-1-1. Functions of LEF1 on lung metastasis ability of the LM8 sublines *in vivo*

In the previous study, adhesion and transmigration assays results have shown that LM8-H has higher extravasation ability than LM8-L *in vitro*. To assess their lung metastatic ability *in vivo*, the LM8 sublines were intravenously injected to mice. BL signal in the lung was significantly higher in the mice injected with LM8-H compared to those injected with LM8-L and LM8-H/*Lef1*-KO cells (Figure 4-1 and 4-2). Consistent with the metastasis results, the extravasation ability to the lung was significantly decreased in LM8-L and LM8-H/*Lef1*-KO1 cells, compared to LM8-H cells (Figure 4-3). These results strongly suggest that the extravasation step could be responsible for differential lung-metastasis abilities of LM8-L and LM8-H cells, and that LEF1 function is indispensable in the extravasation of LM8-H cells to the lungs.

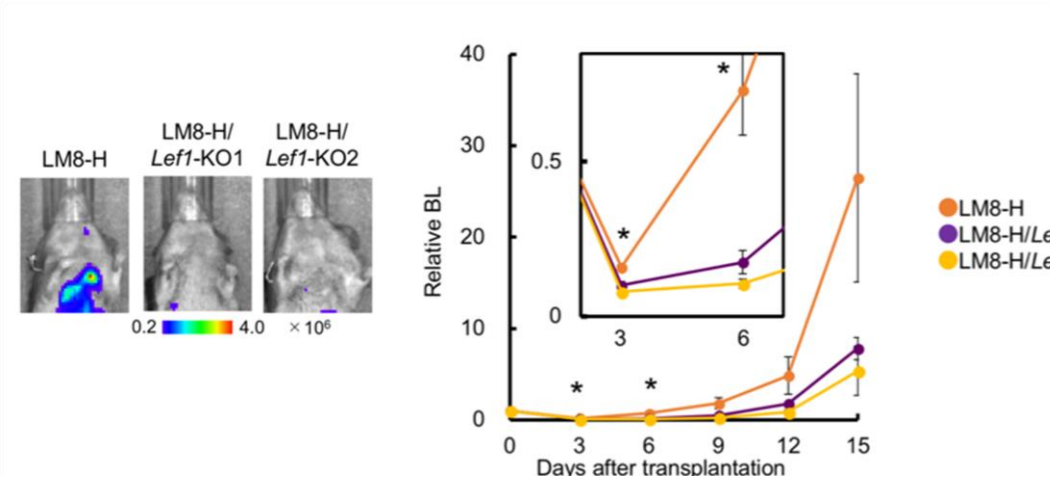

Figure 4-1. Lung-metastatic ability of the LM8-H and LM8-H/*Lef1*-KO sublines. Representative *in vivo* bioluminescence images on day 15 (left) and quantitative analysis of BL signals (right) are shown. The inset graph (right) shows an enlarged view of the images from days 3 and 6. BL signals from the lungs were normalized by those on day 0. n = 3, * $P < 0.05$ (LM8-H vs. LM8-H/*Lef1*-KO1 or LM8-H/*Lef1*-KO2 cells).

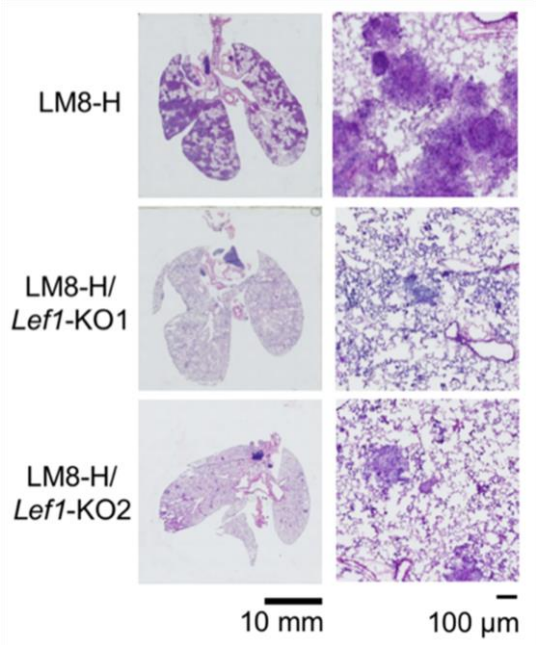

Figure 4-2. Representative HE staining of the lungs at 15 days after intravenous injection of the LM8 sublines.

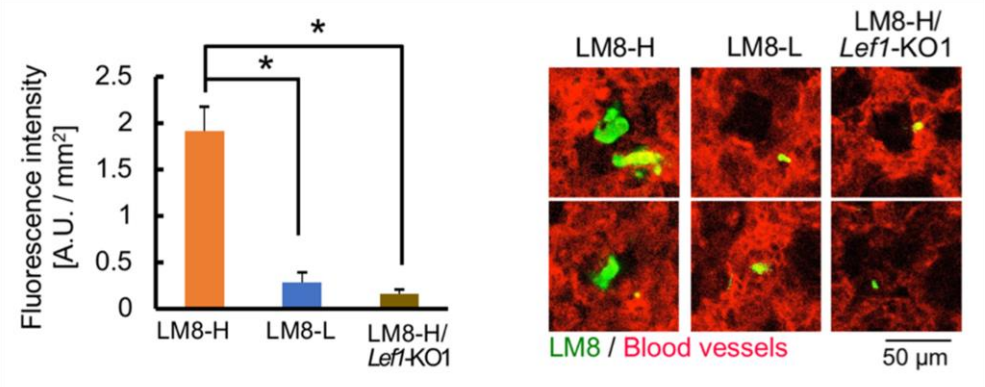

Figure 4-3. Extravasation ability of the LM8 sublines *in vivo*. Quantitative analysis (left) and representative images (right) of the lung 48 h after intravenous injection of the green-fluorescently labelled LM8 sublines. Endothelial cells stained red. n = 9, **P* < 0.05 (vs LM8-H).

4-1-2. Molecular mechanisms of intravasation and extravasation processes

Intravasation and extravasation of cancer cells are requiring the disruption of endothelial junctions for the cancer cells to cross the blood vasculature barrier. For intravasation, tumor cells invade through the tissues towards blood vessels. Tumors induce local angiogenesis, and these new blood vessels generally have weak cell–cell junctions through which cancer cells can enter the vasculature[1]. Some factors reduce endothelial barrier function that promote intravasation ability such as TGF-β or VEGF, increase the number of cancer cells entering into blood vessels[2]. For extravasation, adhesion of cancer-endothelial cell and transmigration processes are critical. After cancer travel to distant organ via blood circulation, cancer cell attached to the vascular endothelial cell by using ligands and receptors recognition between cancer cells and endothelial cells. Several ligands and receptors including selectins, integrins, cadherins, CD44 and immunoglobulin superfamily receptors[3] are related to this process (Figure 4-4A).

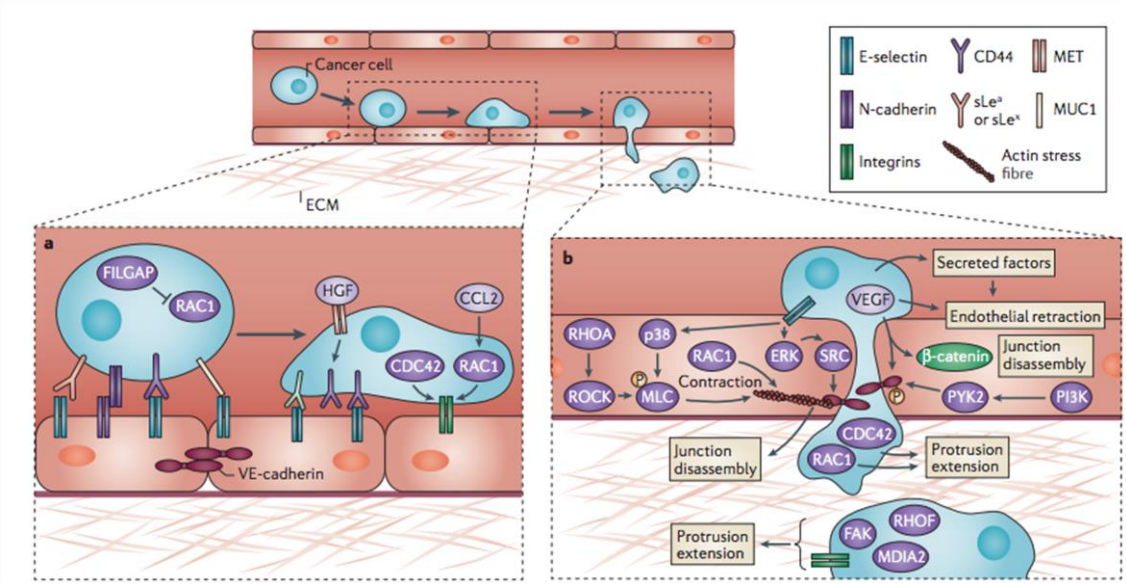

Figure 4-4. Interaction between cancer and endothelial cell during extravasation step. The diagram display summary of interactions during adhesion (a) and transmigration (b) processes. The figure was cited from reference 2.

Variety of adhesion molecules on cancer cells promote their adhesion ability to vascular endothelial cell. The interaction between adhesion molecules are depending on the cancer type and the vascular endothelial cell[3, 4]. Selectins on endothelial cells are important receptors for cancer cell adhesion to endothelial cells by interacting with cell surface

molecules such as tetra-saccharide sialyl Lewis x (sLe^x) antigen or sialyl Lewis a (sLe^a). High expression levels of sLe^x and sLe^a in cancer are correlate with poor prognosis[5]. Ligands for endothelial selectin (E-selectin) are expressed on cancer cells and promote cell adhesion and rolling in many types of cancer by interact with E-selectin (Figure 4-4B). Other molecules including CD44, P-selectin glycoprotein ligand 1, CD24, mucin 1 and galectin-3-binding protein also reported as adhesion molecules overexpressed on cancer cells[6–8].

Then, transmigration process occurs. CDC42 and RAC1 in cancer cells promote transmigration ability in several types of cancer[9, 10]. Wide range of cytokines secreted from cancer cells weaken cell-cell junctions of the vascular endothelial cells by, for example, affecting the binding of αVβ3 integrin to platelet endothelial cell adhesion molecule 1 [3, 11, 12]. In addition, cancer cells induce activation of RAC1, RHOA–RHO-associated protein kinase and p38 MAPK in the endothelial cells. The activation of these pathways increase myosin light chain phosphorylation, stress fiber formation and actomyosin-mediated tension on endothelial cell junctions[3, 12]. In addition, cancer cells activate ERK in the endothelial cell promoting cell junction disassembly[3].

4-2. Materials and methods

4-2-1. Mice

Male BALB/c nu/nu, SCID, and C3H mice were obtained from Charles River Laboratory, Japan (Yokohama, Japan). All mice used were 6 - 8 weeks of age and were housed in the animal facilities at Tokyo Institute of Technology. All experimental producers involving mice were approved by the Animal Experiment Committees of Tokyo Institute of Technology (authorization numbers 2010006 and 2014005) and carried out in accordance with relevant national and international guidelines.

4-2-2. *In vivo* and *ex vivo* BL imaging

Bioluminescence images of mice were acquired using the IVIS® Spectrum system (PerkinElmer, Massachusetts, USA) 15 min after intraperitoneal injection with D-luciferin (50 mg/kg) (Promega, Wisconsin, USA). *Ex vivo* imaging was immediately perfumed after the last *in vivo* image was taken. The following conditions were used for image acquisition: open emission filter, exposure time = 60 s, binning = medium 8, field of view = 12.9 × 12.9 cm, and f/stop = 1. The BL images were analyzed using Living Image 4.3 software (PerkinElmer), developed specifically for the IVIS system.

4-2-3. Lung metastasis assay

C3H mice were intravenously injected with the LM8 sublines (1×10^6 cells/100 μL PBS: 137 mM NaCl; 2.7 mM KCl; 4.3 mM Na_2HPO_4; 1.47 mM KH_2PO_4). Bioluminescence signals from the lungs were monitored through *in vivo* BL imaging on indicated days.

4-2-4. Histology analysis

Isolated lungs were embedded in OCT compound (Sakura Fine Tech, Tokyo, Japan) and stored at –80ºC. Fixed lung cryosections of the lung (10-μm thick) were then stained with HE.

4-2-5. Statistical analysis

Data are presented as the mean ± standard error of the mean and were statistically analyzed with a two-side student's t-test. P values of less than 0.05 were considered statistically significant.

4-3. Results

4-3-1. Functions of CYGB on lung metastasis *in vivo*

In the previous chapter, functions of CYGB in extravasation ability of the LM8 sublines was demonstrated *in vitro*. To assess the function of CYGB in lung metastatic ability of *Cygb*-KO LM8-H (LM8-H/*Cygb*-KO) cells was examined *in vivo*. The LM8 sublines were intravenously injected into C3H mice and BL signals in the lungs were monitored for 16 days. BL imaging results revealed that LM8-H/*Cygb*-KO cells significantly reduced lung metastatic ability compared to LM8-H cells (Figure 4-5).

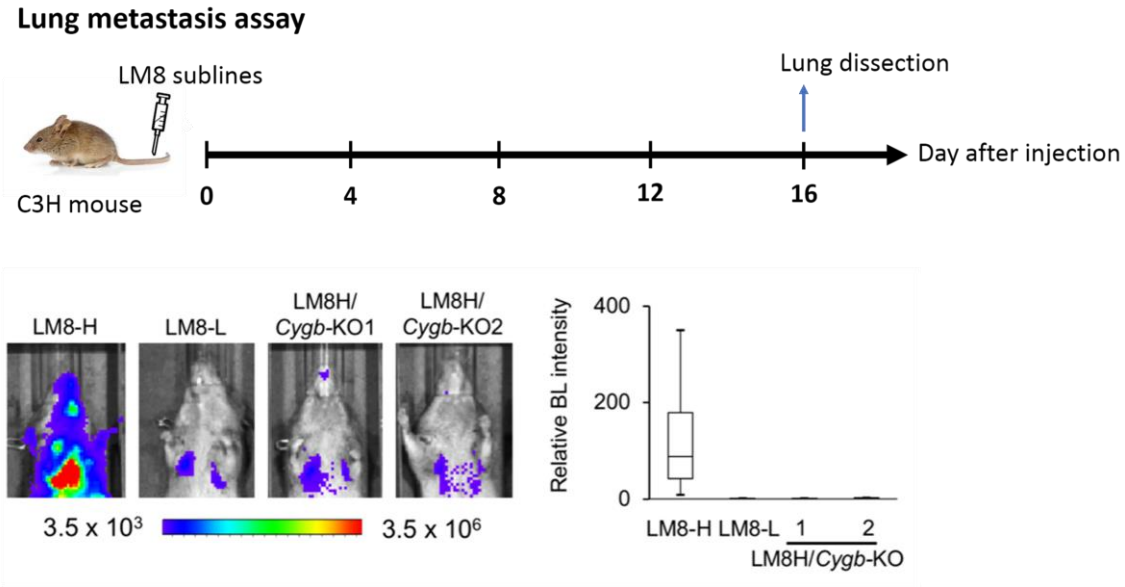

Figure 4-5. Functions of CYGB in lung metastasis. Schematic diagram of lung metastasis assay in syngenic mouse model (top). Bioluminescent images of mice injected with the indicated cells on day 16 (bottom left). Relative BL signals to day 0 are shown in the right box plot (bottom right).

Hematoxylin and eosin (HE) staining of the lungs from mice 16 days after injection of the LM8 sublines confirmed the regulatory function of CYGB in lung metastasis: KO of *Cygb* in LM8-H cells significantly reduced the number of lung metastatic foci (Figure 4-6). The size of foci in the lungs was significantly smaller in the LM8-H/*Cygb*-KO group than the LM8-H group, suggesting that CYGB plays an important role in lung metastasis

in the LM8 sublines (Figure 4-7). In addition, knockout of *Cygb* significantly increased number of cancer cells that trapped inside the lung blood vessels (Figure 4-8).

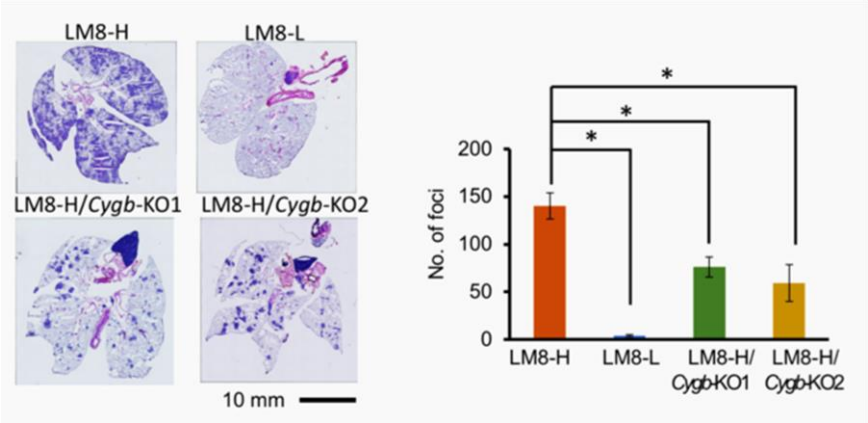

Figure 4-6. Representative HE staining of the lung at 16 days after i.v. injection of LM8 sublines (left). Right graph shows the number of foci in the lung on day 16. n=4 **P*<0.05.

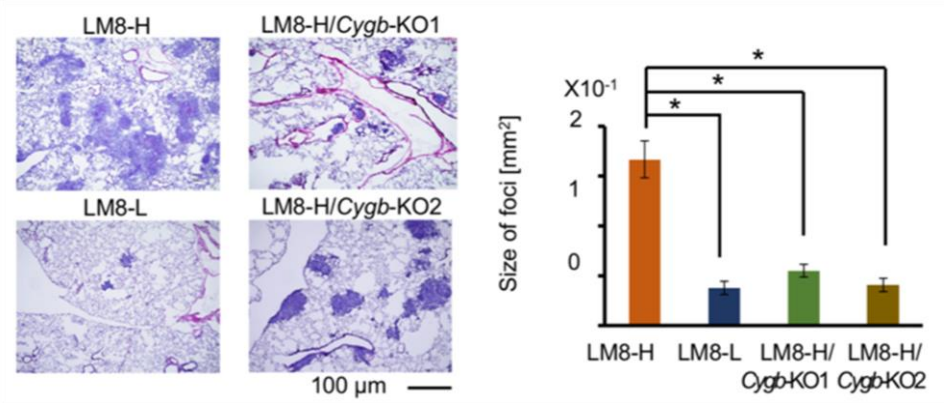

Figure 4-7. Representative HE staining of the lung at 16 days after i.v. injection of LM8 sublines (left). Right graph shows the number of foci in the lung on day 16. n=4 **P*<0.05.

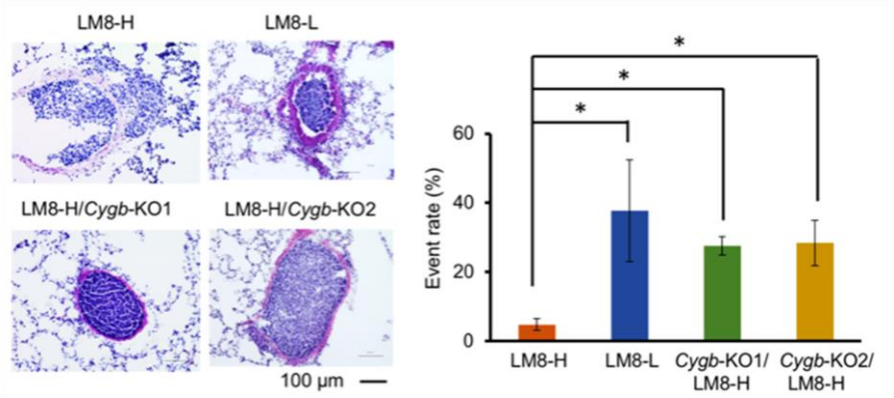

Figure 4-8. Enlarged representative images of metastatic foci of the LM8 sublines on day 16 (Left). Cancer cells trapped in lung vessels on day 16. The percentage of events was calculated using the following formula: Event rate (%) = (number of intravascular foci / total number of foci) x 100. n=4 *P<0.05. (right)

To confirm functions of CYGB in the extravasation ability of the LM8 sublines, extravasation of LM8-H/*Cygb*-KO cells into the lung parenchyma was examined and their residuals in the lung blood vessels was observed (Figure 4-9). These results together with the results of *in vitro* assays support the significance of CYGB function in extravasation in lung metastasis of the LM8 sublines.

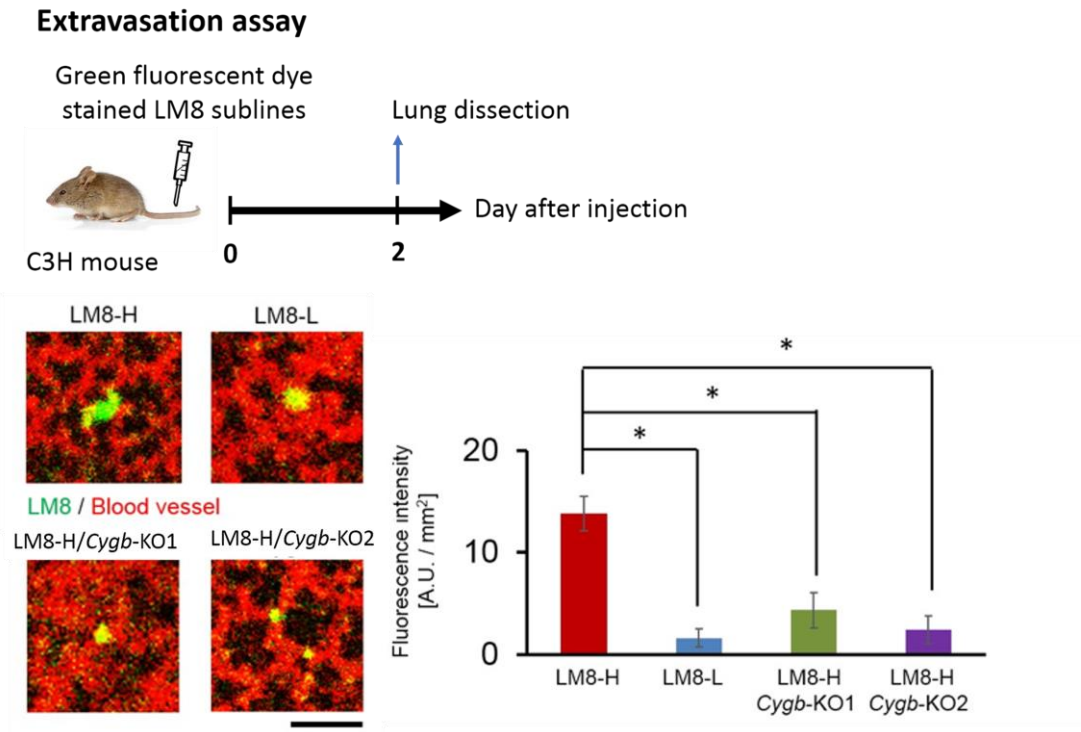

Figure 4-9. CYGB affects extravasation ability of the LM8 sublines. Schematic diagram of the experimental procedures (top). Cancer cells trapped in lung vessels at 48 h after injected LM8 sublines. Representative images (bottom left) and Quantitative analysis (bottom right) of the lung 48 h after intravenous injection of the green-fluorescently labelled LM8 sublines. Endothelial cells stained red. n = 9, *P < 0.05 (vs LM8-H).

Discussion

The KO of *Cygb* in LM8-H cells clearly demonstrated the significance of CYGB in lung metastasis. The number and size of metastatic foci in LM8-H/*Cygb*-KO cells were strongly suppressed, even though the proliferation rate of LM8-H/*Cygb*-KO cells was higher than that of LM8-H cells (Chapter 3). Moreover, LM8-L and LM8-H/*Cygb*-KO cells showed high frequency of staying in the pulmonary blood vessels than LM8-H (Figure 4-8 and Figure 4-9), supporting less extravasation ability of these cells. However, the number of metastatic foci of LM8-H/*Cygb*-KO cells was higher than that of LM8-L cells, suggesting that other downstream effectors of LEF1 also contribute to the lung-metastatic phenotype of LM8-H cells. Furthermore, the ability of adhesion and transmigration (Chapter 3) and the level of *Cygb* expression (Chapter 2) were higher in LM8-H/*Lef1*-KO1 cells than those for LM8-L cells. These results suggest that the expression of *Cygb* could also be regulated by LEF1-independent mechanism.

References

1. Weis SM, Cheresh DA. aV Integrins in Angiogenesis and Cancer. *Cold Spring Harb Perspect Med* 2011; 1: 1–14.
2. Reymond N, d'Agua BB, Ridley AJ. Crossing the endothelial barrier during metastasis. *Nat Rev Cancer* 2013; 13: 858–870.
3. van Zijl F, Krupitza G, Mikulits W. Initial steps of metastasis: Cell invasion and endothelial transmigration. *Mutat Res Mutat Res* 2011; 728: 23–34.
4. Köhler S, Ullrich S, Richter U, et al. E-/P-selectins and colon carcinoma metastasis: first in vivo evidence for their crucial role in a clinically relevant model of spontaneous metastasis formation in the lung. *Br J Cancer* 2009; 102: 602-609.
5. Miles FL, Pruitt FL, Van Golen KL, et al. Stepping out of the flow: Capillary extravasation in cancer metastasis. *Clin Exp Metastasis* 2008; 25: 305–324.
6. Strell C, Entschladen F. Cell Communication and Signaling Extravasation of leukocytes in comparison to tumor cells. *Cell Commun Signal* 2008; 13: 1–13.
7. Shirure VS, Reynolds NM, Burdick MM. Mac-2 Binding Protein Is a Novel E-Selectin Ligand Expressed by Breast Cancer Cells. *PLoS One* 2012; 7: 1–12.
8. Reymond N, Im JH, Garg R, et al. Cdc42 promotes transendothelial migration of cancer cells through β1 integrin. *J Cell Biol* 2012; 199: 653–668.
9. Kazanietz MG, Caloca MJ. The Rac GTPase in cancer: From old concepts to new paradigms. *Cancer Res* 2017; 77: 5445–5451.
10. Katja B, Claudia M, Jürgen B. Expression profiling reveals genes associated with transendothelial migration of tumor cells: A functional role for αvβ3 integrin. *Int J Cancer* 2007; 121: 1910–1918.
11. Kikkawa H, Kaihou M, Horaguchi N, et al. Role of integrin αvβ3 in the early phase of liver metastasis: PET and IVM analyses. *Clin Exp Metastasis* 2002; 19: 717–725.
12. Tan W, Palmby TR, Gavard J, et al. An essential role for Rac1 in endothelial cell function and vascular development. *FASEB J* 2008; 22: 1829–1838.

Chapter 5

Conclusion remarks and future perspectives

Lung metastasis is a major cause of mortality in patients with OS. Surgical and chemotherapeutic strategies have significantly improved survival rate in non-metastatic osteosarcoma patient. However, metastatic disease can prevent long-term cure and decrease 5-year survival rate to 20%. A better understanding of the molecular mechanism of OS lung metastasis may facilitate development of new therapeutic strategies to prevent the metastasis. In the previous work, high (LM8-H) and low (LM8-L) lung metastatic sublines were isolated from murine LM8 osteosarcoma cell line. Molecular genetic analysis of these sublines revealed that *Lef1* has a crucial role in metastatic ability of the LM8 sublines to the lung: Knockdown of *Lef1* totally abolished lung metastasis of LM8 due to reduced extravasation into the lung parenchyma. However, downstream target gene of LEF has not been identified. Thus, I aimed to identify downstream effectors of LEF1 and believed that the data obtained would provide new knowledge and would be useful for developing treatments of OS patients affected with metastasis. To obtain these data, I identified downstream effector genes of LEF1 by using genome-wide meta-analysis to narrow down number of candidate genes. Several of candidate genes were extracted and I found that *Cygb* has good correlation with *Lef1* in transcript levels (Chapter 2). Then, functions of CYGB in lung metastatic ability were assessed *in vitro* and *in vivo* (Chapter 3 and Chapter 4).

Chapter 2 describes the selection of candidate genes using genome-wide meta-analysis by combining microarray data of the LM8 sublines with genomic data sets of human osteosarcoma. This approach successfully narrowed down the candidate genes which might be involved in osteosarcoma lung metastasis. I found that overexpression of some candidate genes were well associated with poor clinical outcome in osteosarcoma patients. These results support that the strategy using genome wide meta-analysis is an efficient method for screening of metastasis associated genes.

Chapter 3 describes functions of CYGB in adhesion and transmigration abilities of the LM8 sublines assessed by *in vitro* assays. Knockout of *Cygb* significantly decreased adhesion and transmigration abilities in LM8-H cell whereas overexpressing of CYGB in LM8-L increased these abilities. These results suggested that CYGB is important for extravasation ability of the LM8 sublines. Total NO and AA levels were not significantly

different among the LM8 sublines. These results suggested that CYGB enhances extravasation ability of the LM8 sublines by using mechanism other than known functions.

Chapter 4 describes functions of CYGB in lung metastasis *in vivo*. Number and size of the foci was significantly smaller in LM8-H/*Cygb*-KO than LM8-H. Moreover, the number of cancer cells trapped inside blood vessel in the lung was significantly higher in LM8-H/*Cygb*-KO than LM8-H. These results suggested that loss of CYGB expression in the cancer cells prevents the cell from extravasating to lung parenchyma and suppresses lung metastasis. These data give new insight into the prevention of metastasis and may be useful in the treatment of metastasis.

The final goal of this study is the identification of key effector genes that regulate lung metastasis in osteosarcoma. In this study, I have identified CYGB as an important regulator of OS extravasation and highlighted the importance of the LEF1-CYGB axis in OS metastasis to the lungs. To my knowledge, this is the first report showing a functional connection between LEF1 and CYGB. However, the mechanism that CYGB regulates the extravasation is still unknown. Since CYGB is localize in cytoplasm and nucleus of the cell, CYGB may interact with transcription factors as a co-factor to increase the expression levels of molecules related to cell adhesion and movement. To prove this hypothesis, localization of CYGB in the LM8 sublines should be investigated.

In addition, gene expression profile and GSEA analysis of CYGB-OE and LM8-H/*Cygb* KO should be analyze. Differential gene expression levels between CYGB-OE and LM8-H/*Cygb*-KO will provide more information about downstream effectors of CYGB that responsible for lung metastasis of the LM8 sublines. Understanding the detailed mechanism how CYGB promotes lung metastasis would provide novel insight for prevention and treatment of lung metastasis.

Achievements

I. Poster presentation

1. Mongkol Pongsuchart, Takahiro Kuchimaru, Tetsuya Kadonosono, Shinae Kondoh, ***In vivo* image-guided screening and genome-wide meta-analysis revealed involvement of LEF1/Cytoglobin axis in lung metastasis of osteosarcoma**, PA-32, The 13th Annual Meeting of The Japanese Society for Molecular Imaging (JSMI 2018), The University of Tokyo Ito International Academic Research Center, **May 2018**

2. Mongkol Pongsuchart, Takahiro Kuchimaru, Tetsuya Kadonosono, Shinae Kondoh, **Identification of genes responsible for osteosarcoma extravasation into the lung**, P-3116, The 76th Annual Meeting of the Cancer Association (JCA 2017), Pacifico Yokohama, **September 2017**

3. Mongkol Pongsuchart, Sakiko Yonezawa, Thi Hong Ngoc Hoang, Takahiro Kuchimaru, Tetsuya Kadonosono, Shinae Kondoh, **Identification of genes regulating osteosarcoma extravasation in lung metastasis**, 3P - 0679, The Molecular Biology Society of Japan Conference (MBSJ 2016), **December, 2016**

4. Mongkol Pongsuchart, Nguyen Kha, Sakiko Yonezawa, Ngoc Hoang, Takahiro Kuchimaru, Tetsuya Kadonosono, Shinae Kondoh, **Identification of responsible genes for osteosarcoma extravasation in lung metastasis by using *in vivo* image-guided system**, O-18, The 11th Annual Meeting of The Japanese Society for Molecular Imaging (JSMI 2016), Kobe International Conference Center, **May 2016**

5. Mongkol Pongsuchart, Nguyen Kha, Sakiko Yonezawa, Ngoc Hoang, Takahiro Kuchimaru, Tetsuya Kadonosono, Shinae Kondoh, **Identification of responsible genes for osteosarcoma extravasation in lung metastasis**, P-1196, The 74th Annual Meeting of the Cancer Association (JCA 2015) Nagoya Congress Center, **October 2015**

II. Published papers

1. Mongkol Pongsuchart, Takahiro Kuchimaru, Sakiko Yonezawa, Diem Thi Phuong Tran, Nguyen The Kha, Ngoc Thi Hong Hoang, Tetsuya Kadonosono, Shinae Kizaka-Kondoh. **A novel lymphoid enhancer-binding factor 1-cytoglobin axis promotes extravasation of osteosarcoma cells into the lungs**. Cancer Science. 2018 (Article in press). doi: 10.1111/cas.13702
2. Mongkol Pongsuchart, Nguyen The Kha, Sakiko Yonezawa, Hoang Thi Hong Ngoc, Takahiro Kuchimaru, Tetsuya Kadonosono, Shinae Kondoh, **Identification of responsible genes for osteosarcoma extravasation in lung metastasis by using *in vivo* image-guided system**. JSMI Report. 2016; 10(1): 61-62

Acknowledgement

I would never have been finished my thesis without the guidance of my academic advisor, the help of members in my lab, and all of my friends. It is my great pleasure to acknowledge people who have guided, helped and encouraged me during the time I studied and conducted the research.

First of all, I would like to express my deepest gratitude to my advisor, Professor Shinae Kondoh. She has helped me so much in devising the original idea of this research. Her endless encouragement has helped me to overcome difficulties in research and daily life. Her enthusiasm and research attitudes have motivated me to keep moving up in academic learning and research.

I am also very grateful to Assistant professor Takahiro Kuchimaru who has supported my research from the beginning. His valuable advice and guidance have helped me improve my research skills. I also have to thank to Assistant professor Tetsuya Kadonosono who gave me enormous valuable discussion and advice.

Additionally, I would also like to thank all of my lab's members for their constant support and discussions for my research. It is my great honor to study and work with them. I also want to thank all my friends who have helped me so much to overcome difficulties in my daily life and academic problems.

I appreciate the mice that I used for this study and express my condolences from the bottom of my heart. I also would like to thank for the Biomaterials Analysis Division of the Tokyo Institute of Technology for DNA sequence analyses and confocal microscope, and Shimadzu Corporation for technical support of AA analysis with LC/MS in Shimadzu corporation precision analytical instruments room of Tokyo Institute of Technology.

In addition, I would like to thank Dr. Ikawa for kindly providing the fluorescence indicator vector pCAG-EGxxFP as a gift.

Mongkol Pongsuchart